

# Analytic treatment of a polaron in a nonparabolic conduction band

S. N. Klimin,<sup>1</sup> J. Tempere,<sup>1,\*</sup> M. Houtput,<sup>1</sup> I. Zappacosta,<sup>1</sup> S. Ragni,<sup>2,†</sup>  
T. Hahn,<sup>3</sup> L. Celiberti,<sup>4</sup> C. Franchini,<sup>4,‡</sup> and A. S. Mishchenko<sup>2,§</sup>

<sup>1</sup>*TQC, Departement Fysica, Universiteit Antwerpen,  
Universiteitsplein 1, B-2610 Antwerpen, Belgium*

<sup>2</sup>*Department for Research of Materials under Extreme Conditions,  
Institute of Physics, 10000 Zagreb, Croatia*

<sup>3</sup>*Center for Computational Quantum Physics, Flatiron Institute,  
162 5th Avenue, New York, New York 10010, USA*

<sup>4</sup>*Faculty of Physics, Computational Materials Physics,  
University of Vienna, Kolingasse 14-16, Vienna A-1090, Austria*

(Dated: March 11, 2026)

# Abstract

We develop and systematically compare several analytical approximations for the polaron problem in finite-width, non-parabolic conduction bands. The main focus of the work is an extension of the Feynman variational method to a tight-binding lattice, where the effective-mass approximation is no longer applicable. The resulting variational formulation is not restricted to a specific phonon dispersion or electron-phonon interaction and provides a uniform description across weak-, intermediate-, and strong-coupling regimes.

In addition, we revisit and generalize other analytical approaches traditionally formulated for continuum polarons, including canonical transformations and self-consistent Wigner-Brillouin-type approximations. For lattice polarons, these methods exhibit qualitative features absent in the continuum case, such as a nontrivial connection between weak- and strong-coupling limits. We show that an improved Wigner-Brillouin scheme yields a momentum-dependent polaron self-energy free of resonances and in good agreement with numerically exact results over the whole range of momenta within the Brillouin zone.

All methods are applied to the Holstein model on a tight-binding lattice and are benchmarked against numerically exact calculations, including Diagrammatic Monte Carlo (both our calculations and preceding works), exact diagonalization, and density-matrix renormalization-group results. Furthermore, the analytical approaches are extended to polarons with Rashba-type spin-orbit coupling, providing a stringent test of their applicability in systems with nontrivial band structure.

Our results demonstrate that the modified Feynman variational method yields ground-state energies and dispersions with accuracy comparable to, and in many cases exceeding, that of other established analytical approaches. The developed framework offers a versatile and reliable analytical description of lattice polarons beyond the continuum approximation.

---

\*Also at Lyman Laboratory of Physics, Harvard University, Cambridge, MA 02138, USA

†Also at Faculty of Physics, Computational Materials Physics, University of Vienna, Kolingasse 14-16, Vienna A-1090, Austria

‡Also at Department of Physics and Astronomy “Augusto Righi”, Alma Mater Studiorum – Università di Bologna, Bologna, 40127 Italy

§Also at RIKEN Center for Emergent Matter Science (CEMS), Wako, Saitama 351-0198, Japan

## I. INTRODUCTION

The polaron, originally introduced by Landau as an electron self-trapped by the polarization field of a crystal lattice [1], constitutes one of the most fundamental and enduring problems in many-body physics. In its most general form, the polaron problem describes a quantum particle interacting with a bosonic field [2–5]. Despite its apparent simplicity, it has resisted an exact analytical solution and has therefore long served as a benchmark problem for the development and testing of analytical approximations and numerical methods [6].

Beyond its conceptual importance, polaron physics plays a central role in a wide range of physical systems in which electron-phonon interactions are not negligible. These include traditional condensed-matter settings such as ionic crystals and molecular solids [7], as well as more recent realizations in ultracold atomic gases [8], polymers [9], and even dense nuclear matter [10]. In parallel with these developments, the scope of polaron physics has broadened considerably, encompassing new types of polarons, nontrivial band structures, and additional couplings such as spin-orbit interaction [11]. As a result, there is a renewed demand for analytical approaches capable of providing both quantitative accuracy and physical transparency across a wide range of parameters.

Over the years, numerous analytical methods have been developed for the polaron problem. In the weak-coupling regime, these include Rayleigh-Schrodinger (RS) perturbation theory and self-consistent approaches such as the Wigner-Brillouin (WB) approximation [12–15]. In the strong-coupling regime, the Lang-Firsov (LF) approximation [16] and the adiabatic (Pekar-type) approximation [17] provide controlled descriptions of small and large polarons, respectively. Other approaches exploit variational ansatzes, coherent phonon states [18, 19], renormalization-group techniques [20], cumulant expansions [21, 22], or canonical transformations (CT) such as the Lee-Low-Pines (LLP) method [23] and its extensions [8].

Among semi-analytical techniques, the momentum-average (MA) approximation [12–14] stands out as one of the most successful methods for lattice polarons with Holstein-type electron-phonon coupling. MA is effective not only for the Holstein polaron. It was applied to Barišić-Labbé-Friedel-Su-Schrieffer-Heeger (BLF-SSH) model [24–27] in Ref. [28], to the breathing model electron-phonon coupling [29] and to other momentum-dependent models [30]. The momentum-average approximation provides remarkably accurate results

for the ground-state energy and spectral properties over a wide parameter range and has been extensively benchmarked against numerically exact methods. However, its accuracy deteriorates in the adiabatic regime when the phonon frequency becomes small compared to the electronic bandwidth, and systematic improvements are required to extend its validity toward the large-polaron limit [14].

A common feature of most analytical approaches is that they are optimized either for a parabolic conduction band of infinite width (continuum polarons) or for specific limiting regimes of lattice models. By contrast, many physically relevant systems are characterized by non-parabolic conduction bands of finite width, where neither the continuum approximation nor purely strong- or weak-coupling treatments are fully adequate. This motivates the search for analytical methods that remain applicable across coupling regimes and bandwidths while retaining quantitative accuracy and conceptual clarity.

The present work is devoted to the systematic development and extension of analytical methods for polarons in finite-width, non-parabolic conduction bands. Focusing primarily on tight-binding lattice models, we generalize several well-known approaches originally formulated for continuum polarons to the lattice case. Particular emphasis is placed on methods that can interpolate between weak- and strong-coupling regimes without ad hoc assumptions.

A central result of this work is an extension of the Feynman variational method [5], originally formulated within the effective-mass approximation, to a tight-binding conduction band of arbitrary width. This generalized Feynman approach is not restricted to a specific form of the electron-phonon interaction or phonon dispersion and naturally encompasses both small- and large-polaron regimes. We show that, for lattice polarons, the modified Feynman variational method yields ground-state energies that are at least as accurate as those obtained from the momentum-average approximation and, in many cases, even closer to numerically exact results.

In parallel, we revisit the method of canonical transformations for lattice polarons. While the Lee-Low-Pines approach is traditionally regarded as a weak-coupling method for continuum polarons, we demonstrate that its extension to finite-width tight-binding bands leads to qualitatively new behavior. Remarkably, the canonical-transformation approach captures not only the weak-coupling limit but also reproduces the correct leading-order strong-coupling (Lang-Firsov) behavior, revealing a nontrivial variational structure absent

in the continuum case.

We also reconsider the self-consistent Wigner-Brillouin approximation, which provides a momentum-dependent polaron self-energy free of resonance divergences. Building on earlier work by Lindemann [31] and by Gerlach and Smondyrev [32], we implement an improved WB scheme (IWB) that exactly reproduces the RS result at zero momentum while yielding a substantially more accurate polaron dispersion throughout the Brillouin zone.

Finally, we extend all considered methods to polarons with Rashba-type spin-orbit coupling. Spin-orbit-coupled polarons provide a stringent test of analytical approaches, as they combine band nonparabolicity, internal spin structure, and electron-phonon interaction on equal footing. We show that both the canonical-transformation method and a reduced Feynman variational approach remain applicable in this context and yield results in good agreement with available numerically exact calculations. For comparison, we refer here to well-established numeric methods: the Diagrammatic Monte Carlo (DiagMC) method applied to a polaron in both parabolic [35] and non-parabolic conduction bands, including preceding works [12, 13] and our own calculation in the present paper; the exact diagonalization and the density-matrix renormalization-group techniques [39–41].

The paper is organized as follows. In Sec. II, we present the formulation and extension of analytical methods for polarons in finite-width tight-binding bands, with and without Rashba spin-orbit coupling. In Sec. III, these methods are applied to lattice polarons, and their predictions for ground-state energies and dispersions are systematically compared with numerically exact results. Section IV summarizes the main findings and outlines perspectives for further developments.

## II. ANALYTIC METHODS

### A. Electron-phonon systems

#### 1. One-band polaron

For a polaron in a single conduction band, we consider an electron–phonon system described by a sufficiently general Hamiltonian with linear interaction, without restrictions on

phonon frequencies and interaction amplitudes,

$$H = \varepsilon(\mathbf{k}) + \sum_{\mathbf{q}} \omega_{\mathbf{q}} \left( b_{\mathbf{q}}^{\dagger} b_{\mathbf{q}} + \frac{1}{2} \right) + \frac{1}{\sqrt{V}} \sum_{\mathbf{q}} V_{\mathbf{q}} e^{i\mathbf{q}\cdot\hat{\mathbf{r}}} \left( b_{\mathbf{q}} + b_{-\mathbf{q}}^{\dagger} \right), \quad (1)$$

where  $\omega_{\mathbf{q}}$  is the phonon frequency and  $V_{\mathbf{q}}$  is the amplitude of the electron–phonon interaction, with phonon creation and annihilation operators  $b_{-\mathbf{q}}^{\dagger}$  and  $b_{\mathbf{q}}$ . The Hamiltonian (1) is written in the momentum representation. We consider the polaron on a linear, square, or cubic lattice (depending on the dimensionality) with lattice constant  $a_0$ . Consequently, the momentum vectors  $\mathbf{k}$  and  $\mathbf{q}$  belong to the reciprocal lattice. Thus, the operator  $e^{i\mathbf{q}\cdot\hat{\mathbf{r}}}$  performs a vector displacement of a  $\mathbf{k}$ -dependent function according to  $e^{i\mathbf{q}\cdot\hat{\mathbf{r}}} f(\mathbf{k}) = f(\mathbf{k} - \mathbf{q})$ .

The band energy in a crystal of dimensionality  $D$  is chosen in the tight-binding form

$$\varepsilon(\mathbf{k}) = -2t \sum_{j=1}^D \cos k_j a_0. \quad (2)$$

The parameter  $t$  characterizes the conduction-band width, which is equal to  $4tD$ . The system volume  $V$  is related to the number of lattice cells  $N$  by  $V = Na_0^D$ , with  $N = L^D$ . In the wide-band limit  $t \gg \omega_{\mathbf{q}}$ , the Hamiltonian (1) describes large continuum polarons. The interaction amplitudes include various types, such as Fröhlich [33], Holstein, etc. In the calculations below, we partly focus on a more specific case, namely the Holstein interaction, with a constant phonon frequency  $\omega_{\mathbf{q}} = \omega_0$  and linear interaction amplitudes given by

$$V_{\mathbf{q}}/\sqrt{V} = g/\sqrt{N}. \quad (3)$$

We also use the dimensionless electron–phonon coupling strength  $\lambda$ , defined following Ref. [12]:

$$\lambda = \frac{1}{D} \frac{g^2}{\omega_0 t}. \quad (4)$$

It should be noted that all derivations in the present work can be straightforwardly reproduced without any change for other polaron types, as long as they can be described by (1) with (2).

## 2. Polaron with the spin-orbit coupling

In the present work, we consider a polaron in two dimensions with Rashba-type spin-orbit coupling [34]. The Hamiltonian for the Rashba polaron in two dimensions follows Ref. [36]:

$$H = \sum_{\mathbf{k}} \begin{pmatrix} c_{\mathbf{k},\uparrow}^\dagger & c_{\mathbf{k},\downarrow}^\dagger \end{pmatrix} \begin{pmatrix} \epsilon(\mathbf{k}) & \phi(\mathbf{k}) \\ \phi^*(\mathbf{k}) & \epsilon(\mathbf{k}) \end{pmatrix} \begin{pmatrix} c_{\mathbf{k}\uparrow} \\ c_{\mathbf{k}\downarrow} \end{pmatrix} + \sum_{\mathbf{q}} \omega_{\mathbf{q}} b_{\mathbf{q}}^\dagger b_{\mathbf{q}} + \frac{g}{\sqrt{N}} \sum_{\mathbf{k},\mathbf{q}} (b_{\mathbf{q}} + b_{-\mathbf{q}}^\dagger) (c_{\mathbf{k}+\mathbf{q},\uparrow}^\dagger c_{\mathbf{k}\uparrow} + c_{\mathbf{k}+\mathbf{q},\downarrow}^\dagger c_{\mathbf{k}\downarrow}). \quad (5)$$

The matrix elements of the free-electron part of the Hamiltonian are

$$\epsilon(\mathbf{k}) = -2t [\cos(k_x a_0) + \cos(k_y a_0)], \quad (6)$$

$$\phi(\mathbf{k}) = 2V_s [i \sin(k_x a_0) + \sin(k_y a_0)]. \quad (7)$$

Without loss of generality, we henceforth consider the case  $V_s \geq 0$ .

For a single polaron, we introduce a spinor state for the electron and rewrite (5), according to the standard correspondence between one-particle and second-quantized operators, in the form

$$H = H_e + \begin{pmatrix} 1 & 0 \\ 0 & 1 \end{pmatrix} \left( \sum_{\mathbf{q}} \omega_{\mathbf{q}} b_{\mathbf{q}}^\dagger b_{\mathbf{q}} + \frac{g}{\sqrt{N}} \sum_{\mathbf{q}} (b_{\mathbf{q}} + b_{-\mathbf{q}}^\dagger) e^{i\mathbf{q}\cdot\hat{\mathbf{r}}} \right), \quad (8)$$

$$H_e = \begin{pmatrix} \epsilon(\mathbf{k}) & \phi(\mathbf{k}) \\ \phi^*(\mathbf{k}) & \epsilon(\mathbf{k}) \end{pmatrix} \quad (9)$$

The matrix Hamiltonian (9) is written in the spin-up and spin-down basis. Since a spin rotation will be used, we describe it explicitly. This unitary transformation is performed using the matrix

$$U = \frac{1}{\sqrt{2}} \begin{pmatrix} -\frac{\sqrt{\phi(\mathbf{k})}}{\sqrt{\phi^*(\mathbf{k})}} & \frac{\sqrt{\phi(\mathbf{k})}}{\sqrt{\phi^*(\mathbf{k})}} \\ 1 & 1 \end{pmatrix}. \quad (10)$$

The transformation (10) diagonalizes the Hamiltonian  $H_e$  and determines the eigenvalues and spinor eigenstates,

$$\varepsilon_{\pm}(\mathbf{k}) = \epsilon(\mathbf{k}) \pm |\phi(\mathbf{k})|, \quad (11)$$

$$u_{\pm} = \frac{1}{\sqrt{2}} \begin{pmatrix} \pm \frac{\sqrt{\phi(\mathbf{k})}}{\sqrt{\phi^*(\mathbf{k})}} \\ 1 \end{pmatrix}. \quad (12)$$

In contrast to the case of an electron in a single band, the band energy of an electron with spin-orbit coupling reaches its minimum at a nonzero momentum. For the tight-binding dispersion laws (6) and (7), the lower spin-split energy band  $\varepsilon_-(\mathbf{k})$  contains four equivalent minima (denoted as  $\mathbf{k}_0$ ) at points in momentum space with components

$$k_{0j} = \pm \frac{1}{a_0} \arctan\left(\frac{V_s}{\sqrt{2}t}\right) \quad (j = x, y). \quad (13)$$

The value of  $\varepsilon_-(\mathbf{k})$  at these points,

$$E_0 \equiv \varepsilon_-(\mathbf{k}_0) = -4t\sqrt{1 + \frac{V_s^2}{2t^2}} \quad (14)$$

is the ground-state energy of a free electron with spin-orbit coupling [41]. The polaron shift of the ground-state energy is measured from  $E_0$ .

## B. Extension of weak-coupling approximations

The main result of the present work is the extension of the Feynman variational method to a polaron in a nonparabolic conduction band of finite width, as described below in Subsec. II C. For reference and comparison, we also consider modifications of other analytic methods that were previously developed for a continuum polaron. These methods are briefly described, with attention paid to how they are altered for a polaron in a tight-binding conduction band, both with and without spin-orbit coupling, relative to the continuum case. As will be seen, their ranges of applicability can also be reassessed in light of these modifications.

### 1. Method of canonical transformations

*a. One-band polaron* We formally exploit the same canonical transformations as in the LLP approach; however, their application to a finite-width, nonparabolic band is nontrivial. The first canonical transformation,

$$S_1 = \exp(-i\mathbf{Q} \cdot \hat{\mathbf{r}}), \quad \mathbf{Q} = \sum_{\mathbf{q}} \mathbf{q} b_{\mathbf{q}}^{\dagger} b_{\mathbf{q}} \quad (15)$$

leads to the Hamiltonian  $\mathcal{H} = S_1^{-1} H S_1$ ,

$$\mathcal{H} = \varepsilon(\mathbf{k} - \mathbf{Q}) + \sum_{\mathbf{q}} \omega_{\mathbf{q}} \left( b_{\mathbf{q}}^{\dagger} b_{\mathbf{q}} + \frac{1}{2} \right) + \frac{1}{\sqrt{V}} \sum_{\mathbf{q}} V_{\mathbf{q}} \left( b_{\mathbf{q}} + b_{-\mathbf{q}}^{\dagger} \right). \quad (16)$$

Because  $\mathcal{H}$  is coordinate-free,  $\mathbf{k} \equiv \mathbf{P}$  is a  $c$ -number vector associated with the total momentum of the electron–phonon system (also referred to as the polaron momentum)  $\mathbf{P}$ .

For a nonparabolic band, the transformation of the electron Hamiltonian is more complicated than in the parabolic case. However, for the tight-binding model it can be carried out analytically, as described in Ref. [38]. We use the known formula [42, 43] involving a matrix  $\mathbb{M} = \|M_{jj'}\|$ ,

$$\exp\left(\sum_{j,j'} b_{j'}^\dagger \mathbb{M}_{jj'} b_{j'}\right) = \mathbb{N} \exp\left(\sum_{j,j'} b_j^\dagger (e^{\mathbb{M}} - 1)_{jj'} b_{j'}\right), \quad (17)$$

where  $\mathbb{N}(\dots)$  denotes normal ordering of creation and annihilation operators. Applying this transformation to the polaron Hamiltonian in a single conduction band with tight-binding dispersion (2), we arrive at the expression used in our work [38]:

$$\begin{aligned} \varepsilon(\mathbf{P} - \mathbf{Q}) = & -t \sum_{j=1}^D \left[ e^{ia_0 P_j} \mathbb{N} \exp\left(\sum_{\mathbf{q}} (e^{-ia_0 q_j} - 1) b_{\mathbf{q}}^\dagger b_{\mathbf{q}}\right) \right. \\ & \left. + e^{-ia_0 P_j} \mathbb{N} \exp\left(\sum_{\mathbf{q}} (e^{ia_0 q_j} - 1) b_{\mathbf{q}}^\dagger b_{\mathbf{q}}\right) \right]. \end{aligned} \quad (18)$$

This expression is still exact. Next, we apply the second canonical transformation,

$$S_2^{-1} = S_2^\dagger = \exp\left[-\sum_{\mathbf{q}} (f_{\mathbf{q}} b_{\mathbf{q}}^\dagger - f_{\mathbf{q}}^* b_{\mathbf{q}})\right], \quad (19)$$

where the functions  $f_{\mathbf{q}}$  are treated as variational parameters and are chosen to minimize the energy.

The trial quantum state within the present approximation exploits the phonon vacuum after the above canonical transformations, defined by the conditions

$$b_{\mathbf{q}} |0_{ph}\rangle = 0, \quad \langle 0_{ph} | b_{\mathbf{q}}^\dagger = 0. \quad (20)$$

Averaging the transformed Hamiltonian with this phonon state, we obtain an extension of the momentum-dependent polaron energy within the CT approximation for a tight-binding conduction band,

$$E^{(CT)}(\mathbf{P}) = \langle 0_{ph} | S_2^{-1} \mathcal{H} S_2 | 0_{ph} \rangle,$$

which is explicitly given by

$$E^{(CT)}(\mathbf{P}) = -2t \operatorname{Re} \sum_{j=1}^D \exp(i a_0 P_j - \Phi_j(\mathbf{P})) + \sum_{\mathbf{q}} \omega_{\mathbf{q}} f_{\mathbf{q}}^* f_{\mathbf{q}} + \frac{1}{\sqrt{V}} \sum_{\mathbf{q}} V_{\mathbf{q}} (f_{\mathbf{q}} + f_{-\mathbf{q}}^*), \quad (21)$$

where we introduce the function

$$\Phi_j(\mathbf{P}) = \sum_{\mathbf{q}} (1 - e^{-i a_0 q_j}) f_{\mathbf{q}}^*(\mathbf{P}) f_{\mathbf{q}}(\mathbf{P}). \quad (22)$$

The optimal values of the phonon shifts  $\{f_{\mathbf{q}}\}$  are obtained by minimizing the polaron energy (21), which results in a closed, finite set of equations for the functions  $\Phi_j(\mathbf{P})$ ,

$$\Phi_j(\mathbf{P}) = \frac{1}{V} \sum_{\mathbf{q}} |V_{\mathbf{q}}|^2 \frac{1 - e^{-i a_0 q_j}}{\Omega_{\mathbf{q}}^2(\mathbf{P})}, \quad (23)$$

with

$$\Omega_{\mathbf{q}}(\mathbf{P}) = \omega_{\mathbf{q}} + 2t \sum_{j=1}^D \operatorname{Re} [e^{i a_0 P_j - \Phi_j(\mathbf{P})} (1 - e^{-i a_0 q_j})]. \quad (24)$$

Thus, instead of an infinite set of equations for  $\{f_{\mathbf{q}}\}$ , we obtain the reduced set (23) for the  $D$  functions  $\{\Phi_j(\mathbf{P})\}$ .

The polaron energy within the CT approach is then obtained using  $f_{\mathbf{q}}(\mathbf{P})$  in the form

$$f_{\mathbf{q}}(\mathbf{P}) = -\frac{1}{\sqrt{V}} \frac{V_{\mathbf{q}}^*}{\Omega_{\mathbf{q}}(\mathbf{P})},$$

which yields the resulting expression for the momentum-dependent polaron self-energy:

$$E^{(CT)}(\mathbf{P}) = -2t \sum_{j=1}^D \operatorname{Re} (e^{i a_0 P_j - \Phi_j(\mathbf{P})}) + \frac{1}{V} \sum_{\mathbf{q}} |V_{\mathbf{q}}|^2 \left( \frac{\omega_{\mathbf{q}}}{\Omega_{\mathbf{q}}^2(\mathbf{P})} - \frac{2}{\Omega_{\mathbf{q}}(\mathbf{P})} \right). \quad (25)$$

Here, the functions  $\Phi_j(\mathbf{P})$  are determined by solving the  $D$ -dimensional set of equations (23).

An analytic check of the polaron self-energy in the continuum limit,  $a_0 \rightarrow 0$ , shows exact agreement with the Lee–Low–Pines result. However, the CT approximation for a polaron with a finite-width band leads to a surprising behavior in the strong-coupling regime. As follows from (23), for sufficiently strong coupling one finds  $\operatorname{Re}(\Phi_j) \gg 1$ . Consequently,  $\Omega_{\mathbf{q}}(\mathbf{P})$  tends to  $\omega_{\mathbf{q}}$ , and the leading strong-coupling contribution to the self-energy becomes

$$E^{(CT,SC)} = -\frac{1}{V} \sum_{\mathbf{q}} \frac{|V_{\mathbf{q}}|^2}{\omega_{\mathbf{q}}}. \quad (26)$$

This expression coincides with the leading term of the Lang–Firsov strong coupling approximation.

In fact, the transition between the weak- and strong-coupling regimes within the CT method is not smooth, because it occurs via a jump between two minima of the variational functional for the self-energy at a certain critical coupling, where the energies of these minima become equal. When approaching the wide-band limit by gradually reducing the lattice constant  $a_0$ ,  $E^{(CT,SC)}$  tends to  $(-\infty)$ , which could suggest a divergence of the polaron energy. This divergence is, however, automatically avoided, because the transition point for the coupling strength shifts to arbitrarily large values as  $a_0$  decreases. As a result, the strong-coupling expression (26) does not appear in the LLP approximation for a continuum polaron.

*b. Polaron with Rashba spin-orbit coupling* For a polaron with spin–orbit coupling, the method from [38] can be extended in the following way. We perform the same canonical transformations as for the single-band polaron and arrive at the polaron energy in matrix form:

$$\mathbb{E}^{(CT)}(\mathbf{P}) = \begin{pmatrix} E_{11}^{(CT)}(\mathbf{P}) & E_{12}^{(CT)}(\mathbf{P}) \\ (E_{12}^{(CT)}(\mathbf{P}))^* & E_{11}^{(CT)}(\mathbf{P}) \end{pmatrix}, \quad (27)$$

with matrix elements

$$E_{11}^{(CT)}(\mathbf{P}) = -2t \operatorname{Re} \sum_{j=x,y} e^{ia_0 P_j - \Phi_j(\mathbf{P})} + \sum_{\mathbf{q}} \left( \omega_{\mathbf{q}} f_{\mathbf{q}}^* f_{\mathbf{q}} + \frac{g}{\sqrt{N}} (f_{\mathbf{q}} + f_{\mathbf{q}}^*) \right), \quad (28)$$

$$E_{12}^{(CT)}(\mathbf{P}) = 2iV_s \operatorname{Im} e^{ia_0 P_x - \Phi_x(\mathbf{P})} + 2V_s \operatorname{Im} e^{ia_0 P_y - \Phi_y(\mathbf{P})}. \quad (29)$$

In the absence of SO splitting,  $V_s = 0$ , the CT polaron energy reduces to the single-band polaron energy (21) multiplied by the identity matrix.

The polaron energy matrix is diagonalized to obtain the eigenvalues and eigenfunctions corresponding to the lower and upper polaron branches. The matrix (27) has the same structure as the bare electron Hamiltonian, and therefore the diagonalization proceeds in exactly the same way. The energy matrix  $\mathbb{E}^{(CT)}(\mathbf{P})$  is thus diagonalized, yielding the spinor eigenfunctions

$$u_{\pm}^{(CT)}(\mathbf{P}) = \frac{1}{\sqrt{2}} \begin{pmatrix} \pm \frac{\sqrt{E_{12}^{(CT)}(\mathbf{P})}}{\sqrt{(E_{12}^{(CT)}(\mathbf{P}))^*}} \\ 1 \end{pmatrix}. \quad (30)$$

The corresponding eigenvalues are given by expressions structurally similar to those for the free electron,

$$E_{\pm}^{(CT)}(\mathbf{P}) = E_{11}^{(CT)}(\mathbf{P}) \pm \left| E_{12}^{(CT)}(\mathbf{P}) \right|. \quad (31)$$

The minimization of the spin-split polaron energies  $E_{\pm}^{(CT)}(\mathbf{P})$  is performed in the same way as for the single-band polaron. As a result, we obtain the set of equations

$$\Phi_j^{\pm}(\mathbf{P}) = \frac{g^2}{N} \sum_{\mathbf{q}} \frac{1 - e^{-ia_0q_j}}{\left[ \Omega_{\mathbf{q}}(\mathbf{P}) \pm \delta\Omega_{\mathbf{q}}^{(SO)}(\mathbf{P}) \right]^2}, \quad (32)$$

with

$$\delta\Omega_{\mathbf{q}}^{(SO)}(\mathbf{P}) = -2V_s \frac{\sum_j \text{Im} \left( e^{ia_0P_j - \Phi_j(\mathbf{P})} \right) \text{Im} \left( e^{ia_0P_j - \Phi_j(\mathbf{P})} (1 - e^{-ia_0q_j}) \right)}{\sqrt{\sum_j \left( \text{Im} e^{ia_0P_j - \Phi_j(\mathbf{P})} \right)^2}}. \quad (33)$$

This quantity can be interpreted as the contribution of spin-orbit coupling to the transition energy.

The optimal values of the polaron self-energies for the spin-split states are obtained from (28) and (29) using the functions  $\Phi_j^{\pm}(\mathbf{P})$ . The explicit expression for the polaron self-energy then reads

$$\begin{aligned} E_{\pm}^{(CT)}(\mathbf{P}) &= -2t \text{Re} \sum_{j=x,y} e^{ia_0P_j - \Phi_j(\mathbf{P})} \\ &+ \frac{g^2}{N} \sum_{\mathbf{q}} \left( \frac{\omega_{\mathbf{q}}}{\left[ \Omega_{\mathbf{q}}(\mathbf{P}) \pm \delta\Omega_{\mathbf{q}}^{(SO)}(\mathbf{P}) \right]^2} - \frac{2}{\Omega_{\mathbf{q}}(\mathbf{P}) \pm \delta\Omega_{\mathbf{q}}^{(SO)}(\mathbf{P})} \right) \\ &\pm 2V_s \sqrt{\sum_j \left( \text{Im} e^{ia_0P_j - \Phi_j(\mathbf{P})} \right)^2}. \end{aligned} \quad (34)$$

According to (32), the optimization of the variational parameters  $f_{\mathbf{q}}$  is performed by minimizing the energy eigenvalues (31) for each eigenstate independently. In other words, each of the two spin-split variational states is adjusted self-consistently. Physically, this independent optimization is closely analogous to that in the well-known variational method for the continuum Fröhlich polaron in the strong-coupling regime, see Refs. [17, 44], where the polaron relaxed excited state (RES) was thoroughly investigated. Similarly to the ground and excited polaron states within the strong-coupling adiabatic approximation, the spinor eigenstates  $u_+^{(CT)}$  and  $u_-^{(CT)}$  are not exactly orthogonal to each other. This allows for a nonradiative relaxation of the upper spin-split polaron state. In contrast to the well-known nonradiative relaxation of a relaxed excited state of a single-band polaron without spin-orbit

coupling [44], the nonradiative transition in the present case occurs with a change of spin projection due to the SO coupling.

## 2. Improved self-consistent Wigner–Brillouin approximation

For reference, we recall the momentum-dependent polaron self-energy within Rayleigh–Schrödinger (RS) perturbation theory, in which the unperturbed states are products of the free-electron wave function  $\Phi_{\mathbf{k}}$  for an electron with momentum  $\mathbf{k}$  and the free-phonon wave function

$$\Psi^{(N_{ph})} = \Phi_{\mathbf{k}} \prod_{\mathbf{q}} |n_{\mathbf{q}}\rangle, \quad (35)$$

where  $N_{ph}$  is the number of phonons,  $N_{ph} = \sum_{\mathbf{q}} n_{\mathbf{q}}$ .

The polaron self-energy within RS perturbation theory is given by

$$E^{(RS)}(\mathbf{k}) = \varepsilon(\mathbf{k}) - \frac{1}{V} \sum_{\mathbf{q}} \frac{|V_{\mathbf{q}}|^2}{\omega_{\mathbf{q}} + \varepsilon(\mathbf{k} - \mathbf{q}) - \varepsilon(\mathbf{k})}. \quad (36)$$

The RS expression is able to reproduce the polaron dispersion only for sufficiently small momenta, because it exhibits resonances when the energy denominator vanishes. Another weak-coupling approximation, the self-consistent Wigner–Brillouin (WB) approximation [32], is free of such resonances but has other shortcomings. Within polaron theory, WB is equivalent to the Tamm–Dankoff (TD) approach [15] and to the self-consistent Born approximation in the Green’s-function formalism [12–14]. The polaron self-energy within WB is determined by

$$E^{(WB)}(\mathbf{k}) = \varepsilon(\mathbf{k}) - \frac{1}{V} \sum_{\mathbf{q}} \frac{|V_{\mathbf{q}}|^2}{\omega_{\mathbf{q}} + \varepsilon(\mathbf{k} - \mathbf{q}) - E^{(WB)}(\mathbf{k})}. \quad (37)$$

Within the TD formalism, the polaron self-energy satisfies a variational inequality and provides an upper bound to the exact polaron self-energy  $E$ ,

$$E \leq E^{(WB)}. \quad (38)$$

An advantage of WB over RS perturbation theory is that WB is free of resonance divergences and therefore yields a qualitatively realistic polaron dispersion. A disadvantage of WB, however, is that it predicts a higher ground-state energy than RS. Since  $E_{pol}^{(WB)}(\mathbf{k}) < \varepsilon(\mathbf{k})$  and  $E_{pol}^{(RS)}(\mathbf{k}) < E_{pol}^{(WB)}(\mathbf{k})$ , in particular  $E_{pol}^{(RS)}(\mathbf{k}) \Big|_{\mathbf{k}=0} < E_{pol}^{(WB)}(\mathbf{k}) \Big|_{\mathbf{k}=0}$ .

This issue was discussed in the literature, notably by G. Lindemann *et al.* [31] and by B. Gerlach and M. A. Smondyrev [32]. In Ref. [31], an elegant procedure was proposed to renormalize WB such that the resulting polaron self-energy at zero momentum exactly coincides with  $E_{pol}^{(RS)}(\mathbf{k})\big|_{\mathbf{k}=0}$ . This is achieved by regrouping terms in the polaron Hamiltonian. For the present problem, the reasoning of Ref. [31] can be slightly rephrased as follows. As discussed by Epstein [45], the decomposition of the total Hamiltonian into unperturbed and perturbed parts is not unique and must be considered separately for each specific problem. In the polaron problem, the ground state ( $\mathbf{k} = 0$ ) is shifted by an amount  $\Delta E_0$ , which lowers the variational ground-state energy. It turns out that the optimal value of this shift, which yields the lowest ground-state energy, is

$$\Delta E_0 = \left( E_{pol}^{(RS)}(\mathbf{k}) - \varepsilon(\mathbf{k}) \right) \bigg|_{\mathbf{k}=0}, \quad (39)$$

which coincides with the choice made in Refs. [31, 32]. It is therefore reasonable, for states with  $\mathbf{k} \neq 0$ , to take this level as the reference for measuring energies. This corresponds to the following decomposition of the Hamiltonian:

$$H = H'_0 + H'_1 = (H_0 + \Delta E_0) + (H_1 - \Delta E_0). \quad (40)$$

We thus start from the unperturbed energy

$$H'_0 \Phi_{\mathbf{k}} |0_{ph}\rangle = (\varepsilon(\mathbf{k}) + \Delta E_0) \Phi_{\mathbf{k}} |0_{ph}\rangle, \quad (41)$$

$$\left( |0_{ph}\rangle \equiv \prod_{\mathbf{q}} |0_{\mathbf{q}}\rangle \right) \quad (42)$$

and solve the Schrödinger equation using a Wigner–Brillouin-type procedure. The first-order perturbation correction compensates the shift  $\Delta E_0$  in (41). Including the second-order energy correction, we obtain a result structurally similar to (37),

$$E_{pol}^{(IWB)}(\mathbf{k}) = \varepsilon(\mathbf{k}) - \frac{1}{V} \sum_{\mathbf{q}} \frac{|V_{\mathbf{q}}|^2}{\omega_{\mathbf{q}} + \varepsilon(\mathbf{k} - \mathbf{q}) + \Delta E_0 - E_{pol}^{(IWB)}(\mathbf{k})}, \quad (43)$$

where the denominator is analogous to that in Eq. (15) of Ref. [31].

As can be seen from (43) together with (39), the self-energy within the improved WB approximation at  $\mathbf{k} = 0$  exactly reproduces the RS perturbation result.

### C. Feynman variational method for a tight-binding polaron

#### 1. Polaron in a single band

*a. Path-integral representation* In this section, we re-derive the phonon influence phase and variational functional in the continuum path-integral representation, but with a non-parabolic kinetic energy for the electron. In the path-integral formalism, thermodynamic potentials (such as the free energy) are calculated via the partition function, which in turn is written as a sum over all possible paths  $\mathbf{r}(\tau)$  of the electron that start and end at the same point, weighted by the exponential factor

$$e^{-\beta F} = \mathcal{Z} = \int \mathcal{D}\mathbf{r} e^{-S[\mathbf{r}(\tau)]}. \quad (44)$$

with the action functional

$$S[\mathbf{r}(\tau)] = \frac{1}{2} \int_0^\beta K_e(\dot{\mathbf{r}}) d\tau - \Phi[\mathbf{r}(\tau)]. \quad (45)$$

Here  $\mathbf{r}(\tau)$  is the electron path expressed in imaginary time, yielding the Euclidean action, and  $\beta = 1/(k_B T)$ , where  $T$  is the temperature. The kinetic energy  $K_e(\dot{\mathbf{r}})$  appears after integrating the phase-space path integral over the electron momenta. For a nonparabolic conduction band with dispersion  $\varepsilon(\hat{\mathbf{p}})$ , the explicit analytic form of  $K_e(\dot{\mathbf{r}})$  is not known. However, as shown below, this knowledge is not required, because the kinetic energy does not enter explicitly into the final expressions.

The influence phase corresponding to (1) has the well-known form [5]:

$$\begin{aligned} \Phi[\mathbf{r}(\tau)] &= \frac{1}{2} \sum_{\mathbf{q}} \frac{|V_{\mathbf{q}}|^2}{V} \int_0^\beta d\tau \int_0^\beta d\tau' e^{i\mathbf{q} \cdot (\mathbf{r}(\tau) - \mathbf{r}(\tau'))} \\ &\times \frac{\cosh \omega_{\mathbf{q}} (|\tau - \tau'| - \frac{1}{2}\beta)}{\sinh \frac{1}{2}\beta \omega_{\mathbf{q}}}. \end{aligned} \quad (46)$$

Following Feynman, the variational method proposed here considers a *partly quadratic* trial action in which the phonon degrees of freedom are replaced by a fictitious particle with coordinate  $\mathbf{r}_f(\tau)$  and quadratic kinetic energy,

$$S_{tr}[\mathbf{r}(\tau), \mathbf{r}_f(\tau)] = \int_0^\beta \left( K_e(\dot{\mathbf{r}}) + \frac{m_f \dot{\mathbf{r}}_f^2}{2} + \frac{m_f w^2}{2} (\mathbf{r}_f - \mathbf{r})^2 \right) d\tau, \quad (47)$$

where the fictitious particle interacts harmonically with the electron.

The partition function corresponding to this model is

$$\mathcal{Z}_{tr} = \int \mathcal{D}\mathbf{r} \int \mathcal{D}\mathbf{r}_f e^{-S_{tr}[\mathbf{r}(\tau), \mathbf{r}_f(\tau)]}. \quad (48)$$

Expectation values of functionals  $\mathcal{F}[\mathbf{r}(\tau)]$  of the electron path are given by

$$\begin{aligned} \langle \mathcal{F}[\mathbf{r}(\tau)] \rangle_{tr} &= \frac{1}{\mathcal{Z}_{tr}} \int \mathcal{D}\mathbf{r} \mathcal{F}[\mathbf{r}(\tau)] \\ &\times \int \mathcal{D}\mathbf{r}_f e^{-S_{tr}[\mathbf{r}(\tau), \mathbf{r}_f(\tau)]}. \end{aligned} \quad (49)$$

It is evident that performing the path integral over  $\mathbf{r}_f$  exactly simplifies the result. The outcome of this integration still depends on the path  $\mathbf{r}(\tau)$  and can be expressed in terms of an influence phase describing a quadratic retarded interaction for the electron. The partition function of the model system becomes

$$\begin{aligned} \mathcal{Z}_{tr} &= \mathcal{Z}_f \int \mathcal{D}\mathbf{r} \exp \left\{ - \int_0^\beta K_e(\dot{\mathbf{r}}) d\tau + \Phi_0[\mathbf{r}(\tau)] \right\} \\ &= \mathcal{Z}_f \int \mathcal{D}\mathbf{r} \exp \{ -S_0[\mathbf{r}(\tau)] \}, \end{aligned} \quad (50)$$

with the retarded action

$$S_0[\mathbf{r}(\tau)] = \int_0^\beta K_e(\dot{\mathbf{r}}) d\tau - \Phi_0[\mathbf{r}(\tau)] \quad (51)$$

and the partition function of the fictitious particle

$$\mathcal{Z}_f = \int \mathcal{D}\mathbf{r}_f \exp \left\{ - \int_0^\beta \left[ \frac{m_f \dot{\mathbf{r}}_f^2}{2} + \frac{m_f w^2}{2} \mathbf{r}_f^2 \right] d\tau \right\}. \quad (52)$$

Feynman restricted the trial action to a quadratic form, since only in this case can the influence phase be calculated analytically, and obtained

$$\begin{aligned} \Phi_0[\mathbf{r}(\tau)] &= -\frac{m_f w^3}{4} \int_0^\beta d\tau \int_0^\beta d\tau' [\mathbf{r}(\tau) - \mathbf{r}(\tau')]^2 \\ &\times \frac{\cosh \left[ w \left( |\tau - \tau'| - \frac{\beta}{2} \right) \right]}{\sinh(\beta w/2)}. \end{aligned} \quad (53)$$

Using Jensen's inequality

$$\langle e^{\mathcal{F}[\mathbf{r}(\tau)]} \rangle \geq e^{\langle \mathcal{F}[\mathbf{r}(\tau)] \rangle}, \quad (54)$$

and taking the logarithm leads to the variational inequality for the free energy,

$$F \leq F_{tr} - F_f + \frac{1}{\beta} \langle \Phi_0 [\mathbf{r}(\tau)] \rangle_0 - \frac{1}{\beta} \langle \Phi [\mathbf{r}(\tau)] \rangle_0. \quad (55)$$

In the zero-temperature limit, this yields the variational inequality for the ground-state energy,

$$E^{(GS)} \leq E_{tr}^{(0)} - E_f^{(0)} + \lim_{\beta \rightarrow \infty} \frac{1}{\beta} \langle \Phi_0 [\mathbf{r}(\tau)] \rangle_0 - \lim_{\beta \rightarrow \infty} \frac{1}{\beta} \langle \Phi [\mathbf{r}(\tau)] \rangle_0. \quad (56)$$

The averaged influence phase of phonons can be simplified by reducing the number of integrations using the symmetry properties of the correlation function [5]. After the standard change of variables, we arrive at the following expression for the averaged influence phase:

$$\frac{1}{\beta} \langle \Phi \rangle_0 = \sum_{\mathbf{q}} \frac{|V_{\mathbf{q}}|^2}{V} \int_0^{\beta/2} d\tau \langle e^{i\mathbf{q}\cdot\mathbf{r}(\tau)} e^{-i\mathbf{q}\cdot\mathbf{r}(0)} \rangle_0 \frac{\cosh \omega_{\mathbf{q}} (\tau - \frac{1}{2}\beta)}{\sinh \frac{1}{2}\beta\omega_{\mathbf{q}}}. \quad (57)$$

The averaged influence phase of the fictitious particle is derived in the same way and reads

$$\frac{1}{\beta} \langle \Phi_0 [\mathbf{r}(\tau)] \rangle_0 = -\frac{m_f w^3}{2} \int_0^{\beta/2} d\tau \langle [\mathbf{r}(\tau) - \mathbf{r}(0)]^2 \rangle_0 \frac{\cosh [w (\tau - \frac{\beta}{2})]}{\sinh(\beta w/2)}. \quad (58)$$

In the particular case  $T = 0$ , we obtain

$$\lim_{\beta \rightarrow \infty} \frac{1}{\beta} \langle \Phi_0 [\mathbf{r}(\tau)] \rangle_0 = -\frac{m_f w^3}{2} \int_0^{\infty} d\tau e^{-w\tau} \langle [\mathbf{r}(\tau) - \mathbf{r}(0)]^2 \rangle_0. \quad (59)$$

The averages in (58) and (59) can be expressed in terms of the same correlation function that appears in the averaged influence phase of phonons:

$$\langle [\mathbf{r}(\tau) - \mathbf{r}(0)]^2 \rangle_0 = -\frac{\partial^2}{\partial \mathbf{q}^2} \langle e^{i\mathbf{q}\cdot\mathbf{r}(\tau)} e^{-i\mathbf{q}\cdot\mathbf{r}(0)} \rangle_0 \Big|_{\mathbf{q}=0}. \quad (60)$$

*b. Eigenstates of the trial system* The path-integral formalism was used above solely because it allows a shorter and more transparent presentation of the derivations compared to the language of ordered operators. Further on, we switch to the operator representation, in which operator products appearing in correlation functions are ordered along the axis of thermodynamic “time”  $\tau$ . The operator and path-integral representations are equivalent: the ordering of points on the Euclidean time axis in the path-integral formalism corresponds to time ordering in the operator formulation. Accordingly, the expressions for the variational polaron energy have the same form in both representations [46].

As shown above, the variational polaron energy can be expressed in terms of the retarded interaction that appears after exact averaging of the electron–phonon density matrix over states of the phonon subsystem, or, equivalently, in the path-integral formalism, after integration over phonon paths. The averaging in the correlation functions entering the variational functional is performed using the eigenfunctions of the trial Hamiltonian, which in the momentum representation reads

$$H_{tr} = \varepsilon(\mathbf{k}) + \frac{\mathbf{k}_f^2}{2m_f} + \frac{m_f w^2}{2} (\hat{\mathbf{r}} - \hat{\mathbf{r}}_f)^2. \quad (61)$$

The averages in the variational functional for the polaron self-energy are calculated with the eigenfunctions of the trial Hamiltonian (61). To be consistent with the exact polaron model in a tight-binding conduction band in  $D$  dimensions described above, both  $\mathbf{k}$  and  $\mathbf{k}_f$  are defined on a lattice with inverse lattice constant  $2\pi/(a_0L)$ . The momentum  $\mathbf{k}$  is restricted to the first Brillouin zone,  $-\pi/a_0 \leq k_j < \pi/a_0$  ( $j = 1, \dots, D$ ), with periodic boundary conditions. The momentum space associated with  $\mathbf{k}_f$  is infinite, in accordance with the model of a particle with a parabolic dispersion confined by a harmonic potential.

We perform the transformation of coordinates and momenta

$$\begin{cases} \hat{\mathbf{r}}_c = a\hat{\mathbf{r}} + (1-a)\hat{\mathbf{r}}_f \\ \boldsymbol{\rho} = \hat{\mathbf{r}} - \hat{\mathbf{r}}_f \end{cases}, \quad \begin{cases} \mathbf{k}_c = \mathbf{k} + \mathbf{k}_f \\ \mathbf{k}_\rho = (1-a)\mathbf{k} - a\mathbf{k}_f \end{cases}, \quad (62)$$

with a real parameter  $a$ . This transformation is unitary for any value of  $a$ . Moreover, one can always perform an additional unitary transformation  $e^{-iak_c \cdot \hat{\boldsymbol{\rho}}}$ , such that the resulting Hamiltonian is equivalent to that obtained by choosing  $a = 0$ . Consequently, the Hamiltonian (61) expressed in the new variables takes the form

$$H_{tr} = \varepsilon(\mathbf{k}_\rho) + \frac{(\mathbf{k}_\rho - \mathbf{k}_c)^2}{2m_f} - \frac{m_f w^2}{2} \frac{\partial^2}{\partial \mathbf{k}_\rho^2}. \quad (63)$$

The Hamiltonian (63) does not contain the coordinate  $\hat{\mathbf{r}}_c$ . Hence, the momentum  $\mathbf{k}_c$  is conserved and, according to  $\mathbf{k}_c = \mathbf{k} + \mathbf{k}_f$  in (62), coincides with the total momentum of the trial system. This quantity can be identified with the total polaron momentum  $\mathbf{P}$  within the present approximation. The eigenfunctions of  $H_{tr}$  with  $\mathbf{k}_c = \mathbf{P}$  are denoted  $\varphi_{\mathbf{P}}^{(n)}(\mathbf{k}_\rho)$  and satisfy

$$\left[ \varepsilon(\mathbf{k}_\rho) + \frac{(\mathbf{k}_\rho - \mathbf{P})^2}{2m_f} - \frac{m_f w^2}{2} \frac{\partial^2}{\partial \mathbf{k}_\rho^2} \right] \varphi_{\mathbf{P}}^{(n)}(\mathbf{k}_\rho) = \varepsilon_{\mathbf{P}}^{(n)} \varphi_{\mathbf{P}}^{(n)}(\mathbf{k}_\rho). \quad (64)$$

The energy levels of the fictitious particle, which also enter the variational functional, are obtained from (52) as solutions of

$$\left( \frac{\mathbf{k}^2}{2m_f} - \frac{m_f w^2}{2} \frac{\partial^2}{\partial \mathbf{k}^2} \right) \varphi_f^{(n)}(\mathbf{k}) = \varepsilon_f^{(n)} \varphi_f^{(n)}(\mathbf{k}). \quad (65)$$

As can be seen from Eqs. (64) and (65), if  $\mathbf{k}$  was interpreted as a position variable, these equations would be equivalent to the real-space Schrödinger equation for a particle with an effective mass  $1/(m_f w^2)$ . They can be solved numerically exactly by diagonalizing the trial Hamiltonian on a momentum-space lattice, which constitutes an advantage of employing the momentum representation for practical calculations.

*c. Variational functional* After substitution of the trial eigenfunctions and energies, the zero-temperature self-energy within the modified Feynman approximation takes the form:

$$E_{pol}^{(F)}(\mathbf{P}) = \varepsilon_{\mathbf{P}}^{(0)} - \varepsilon_f^{(0)} + \lim_{\beta \rightarrow \infty} \frac{1}{\beta} \langle \Phi_0 \rangle_0 - \lim_{\beta \rightarrow \infty} \frac{1}{\beta} \langle \hat{\Phi} \rangle_0, \quad (66)$$

where the last term represents the contribution due to the electron-phonon interaction,

$$\lim_{\beta \rightarrow \infty} \frac{1}{\beta} \langle \hat{\Phi} \rangle_0 = \sum_{\mathbf{q}} \frac{|V_{\mathbf{q}}|^2}{V} \sum_n \frac{|\sum_{\mathbf{k}} (\varphi_{\mathbf{P}}^{(0)}(\mathbf{k}))^* \varphi_{\mathbf{P}+\mathbf{q}}^{(n)}(\mathbf{k} + \mathbf{q})|^2}{\omega_{\mathbf{q}} + \varepsilon_{\mathbf{P}+\mathbf{q}}^{(n)} - \varepsilon_{\mathbf{P}}^{(0)}}. \quad (67)$$

The averaged influence phase of the fictitious particle is obtained in an explicit form by disentangling operator exponents in the correlation function  $\langle e^{i\mathbf{q}\cdot\mathbf{r}(\tau)} e^{-i\mathbf{q}\cdot\mathbf{r}(0)} \rangle_0$  and subsequently expanding in a Taylor series in  $\mathbf{q}$ . This procedure allows one to avoid a numerical evaluation of derivatives in momentum space in (60) in the limit  $\mathbf{q} \rightarrow 0$ . As a result, we obtain

$$\begin{aligned} \lim_{\beta \rightarrow 0} \frac{1}{\beta} \langle \Phi_0 \rangle_0 = m_f w \left( 2t^2 a_0^2 \sum_{j=1}^D \sum_n \frac{|\langle \varphi_{\mathbf{P}}^{(0)} | \sin(k_j a_0) | \varphi_{\mathbf{P}}^{(n)} \rangle|^2}{w + \varepsilon_{\mathbf{P}}^{(n)} - \varepsilon_{\mathbf{P}}^{(0)}} \right. \\ \left. - \frac{1}{2} t a_0^2 \sum_{j=1}^D \langle \varphi_{\mathbf{P}}^{(0)} | \cos(k_j a_0) | \varphi_{\mathbf{P}}^{(0)} \rangle \right). \end{aligned} \quad (68)$$

The variational parameters  $m_f$  and  $w$  for the polaron self-energy are obtained using the variational inequality, which is substantiated for the ground state, i.e., for zero polaron momentum:

$$E^{(GS)} \leq E_{pol}(\mathbf{P})|_{\mathbf{P}=0}, \quad (69)$$

where  $E^{(GS)}$  is the exact polaron ground-state energy.

*d. Reduced Feynman approximation* A simpler upper bound for the polaron energy can be derived without resorting to an exact average of the trial influence phase. It is obtained by setting the mass  $m_f$  of the fictitious particle to  $m_f \rightarrow \infty$ . Within this approximation, the variational polaron self-energy follows directly from Eq. (61), in a more transparent manner than by taking the limiting procedure in the averaged influence phase of the trial system (68). In this limit, the trial Hamiltonian reduces to that of an electron in a static parabolic potential, and the polaron self-energy is obtained without any retarded action in the trial system. Thus, one arrives at the variational functional,

$$E_{pol}^{(RF)} = \left\langle \varphi_0^{(0)} \left| \varepsilon(\mathbf{k}) \right| \varphi_0^{(0)} \right\rangle - \lim_{\beta \rightarrow \infty} \frac{1}{\beta} \left\langle \varphi_0^{(0)} \left| \hat{\Phi} \right| \varphi_0^{(0)} \right\rangle, \quad (70)$$

which results in the expression

$$E_{pol}^{(RF)} = \left\langle \varphi_0^{(0)} \left| \varepsilon(\mathbf{k}) \right| \varphi_0^{(0)} \right\rangle - \sum_{\mathbf{q}} \frac{|V_{\mathbf{q}}|^2}{V} \sum_n \frac{\left| \sum_{\mathbf{k}} \left( \varphi_0^{(0)}(\mathbf{k}) \right)^* \varphi_0^{(n)}(\mathbf{k} + \mathbf{q}) \right|^2}{\omega_{\mathbf{q}} + \varepsilon_0^{(n)} - \varepsilon_0^{(0)}}, \quad (71)$$

where the momentum dependence of the variational self-energy flattens to a constant,  $\mathbf{P}$ -independent value. Here the trial eigenfunctions  $\varphi_0^{(n)}(\mathbf{k}) \equiv \lim_{m_f \rightarrow \infty} \varphi_{\mathbf{P}}^{(n)}(\mathbf{k})$  and energies  $\varepsilon_0^{(n)} \equiv \lim_{m_f \rightarrow \infty} \varepsilon_{\mathbf{P}}^{(n)}$  are defined in the corresponding limit. This approximation can be referred to as the reduced Feynman (RF) variational approach or, equivalently, as an improved strong coupling approximation. The strong-coupling adiabatic approximation is recovered from (71) by retaining only the  $n = 0$  term in the sum over quantum numbers. Therefore, (71) indeed improves upon the strong coupling adiabatic ansatz and yields a lower variational polaron energy. However, the variational functional within the reduced Feynman approximation,  $E_{pol}^{(RF)}$ , is unable to describe the momentum dependence of the polaron energy and cannot lie below  $E_{var}$  given by (56), because the limit  $m_f \rightarrow \infty$  is, in general, not an optimal choice.

Despite the fact that the full variational expression for the polaron self-energy is available, the reduced Feynman approximation is also of interest, especially for polarons with spin-orbit coupling, because its extension to the spin-orbit coupled case is rigorously justified, whereas the full Feynman variational method requires a further analysis of the validity of the variational principle for a complex Hamiltonian. Additionally, it is much less time-consuming to evaluate in practice. Indeed, the trial eigenfunctions  $\varphi_{\mathbf{P}}^{(n)}(\mathbf{k})$  must only be evaluated at a single momentum  $\mathbf{P}$ , which requires only one solution of the Schrödinger-like equation in (64). This is in contrast to the full Feynman variational method, which requires solving this equation for every value of  $\mathbf{P}$ .

Remarkably, the reduced Feynman approximation exactly reproduces both the strong-coupling and weak-coupling limits of (56) for the ground-state energy, and predicts only slightly higher values than the full Feynman approach in the intermediate coupling regime. The successful application of the reduced Feynman approximation in the weak-coupling regime may appear counterintuitive at first sight, but it follows from the completeness of the set of eigenstates  $\{\varphi_0^{(n)}(\mathbf{k})\}$ .

## 2. Polaron with spin-orbit coupling

In the present work, we apply the reduced Feynman variational approach to the spin-orbit coupled polaron in a tight-binding conduction band, as described by (8) and (9) together with (6) and (7). The full Feynman approach is also applicable to this problem, but it requires a rigorous justification of the variational principle, because the electron-phonon system is described by a complex matrix Hamiltonian which might invalidate the Jensen inequality. In contrast, the reduced Feynman approach is in fact based on the Ritz variational principle, which is valid for any Hermitian Hamiltonian. Indeed, the limiting transition  $m_f \rightarrow +\infty$  reduces the trial Hamiltonian (63) to one with a static quadratic interaction. As a consequence, no retarded interaction with the fictitious particle appears in the variational functional. With respect to the averaged retarded interaction with phonons, the same term as in Ref. [47] is employed, where it is shown that the Ritz variational principle can be applied to a system describing an electron with a retarded self-interaction generated by the electron-phonon interaction.

For a polaron with spin-orbit coupling, we employ the following trial Hamiltonian:

$$H_{tr} = \begin{pmatrix} \epsilon(\mathbf{k}) & \phi(\mathbf{k}) \\ \phi^*(\mathbf{k}) & \epsilon(\mathbf{k}) \end{pmatrix} - \frac{\varpi^2}{2} \begin{pmatrix} 1 & 0 \\ 0 & 1 \end{pmatrix} \frac{\partial^2}{\partial \mathbf{k}^2}, \quad (72)$$

with variational parameter  $\varpi$ . The eigenvalues  $\varepsilon_n$  and the two-dimensional spinor eigenfunctions  $u_n(\mathbf{k})$  are determined from

$$H_{tr}u_n(\mathbf{k}) = \varepsilon_n u_n(\mathbf{k}). \quad (73)$$

This equation is solved numerically exactly in the same manner as above, by exact diagonalization of the Hamiltonian (72) on a momentum-space lattice. The only difference with respect to the reduced Feynman approach for a single-band polaron is the spinor, rather than

scalar, form of the trial Hamiltonian. Consequently, the resulting variational functional for the polaron self-energy  $E_{var}^{(SO)}$  is given by an expression analogous to (71), using the obtained energy eigenvalues and spinor eigenfunctions:

$$E_{pol}^{(RF)} = \sum_{\mathbf{k}} u_0^\dagger(\mathbf{k}) \cdot \begin{pmatrix} \epsilon(\mathbf{k}) & \phi(\mathbf{k}) \\ \phi^*(\mathbf{k}) & \epsilon(\mathbf{k}) \end{pmatrix} \cdot u_0(\mathbf{k}) - \sum_{\mathbf{q}} \frac{|V_{\mathbf{q}}|^2}{V} \sum_n \frac{|\sum_{\mathbf{k}} u_0^\dagger(\mathbf{k}) \cdot u_n(\mathbf{k} + \mathbf{q})|^2}{\omega_{\mathbf{q}} + \epsilon_n - \epsilon_0}. \quad (74)$$

For the subsequent numerical calculations, we employ nondispersive optical phonons with frequency  $\omega_{\mathbf{q}} = \omega_0$  and the Holstein electron–phonon interaction described by (3) and (4).

### III. RESULTS AND DISCUSSION

#### A. Polaron ground state energy

##### 1. Single band

In Fig. 1, we plot the ground-state energy of a Holstein polaron in 1D as a function of the coupling constant  $\lambda$  for  $\omega_0 = 0.5t$ , calculated using the modified Feynman variational method described above, both full and reduced versions. The result is compared with Rayleigh–Schrödinger (RS) perturbation theory, our Diagrammatic Monte Carlo results and those of Refs. [12, 13], the momentum-average approximation [12–14], and the method of canonical transformations.

In the numerical evaluation of the polaron self-energy using the full modified Feynman variational method with the averaged influence phase (68), one technical point arises. This issue follows from (59), which is asymptotically exact in the limit  $N \rightarrow \infty$ . In the weak-coupling limit at  $N \rightarrow \infty$ , the variational ground-state energy analytically tends to the result of RS perturbation theory, analogously to the weak-coupling regime of the continuum polaron within the Feynman variational method [5]. For finite  $N$ , the resulting self-energy is numerically reliable as long as the radius of the polaron ground state remains much smaller than the system size.

In the weak-coupling limit the polaron extends over the entire crystal. As  $\lambda \rightarrow 0$ , the above condition ceases to hold, and the variational functional loses stability when  $\lambda$  becomes

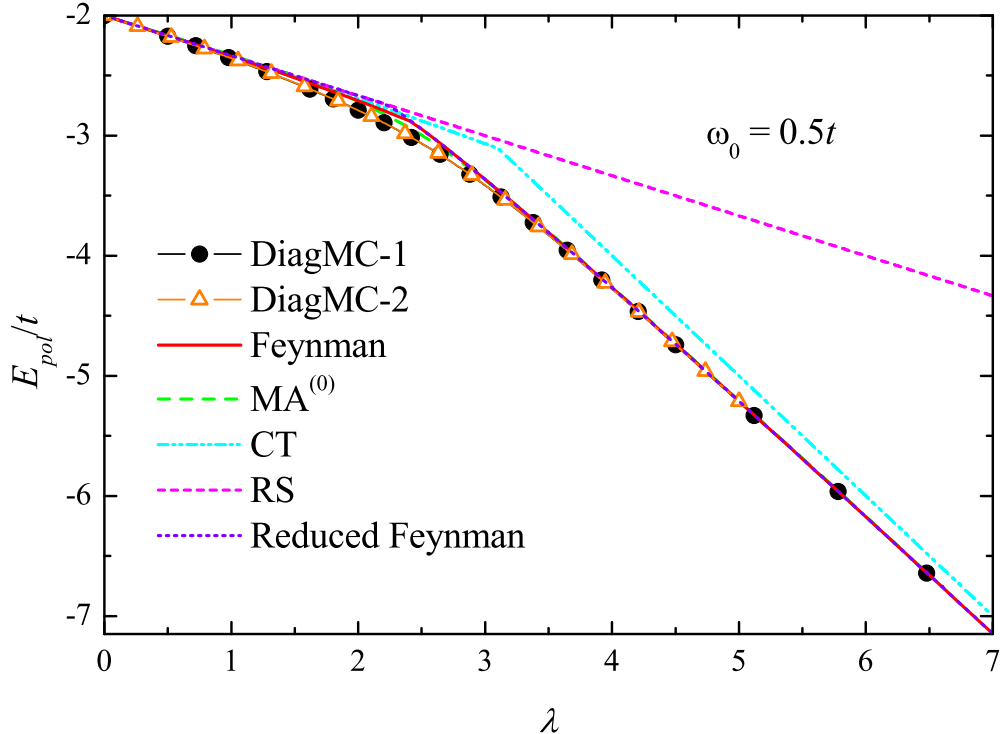


FIG. 1: Ground state energy of a Holstein polaron in 1D for  $\omega_0 = 0.5t$ , calculated by different methods: Diagrammatic Monte Carlo [12, 13] (*full dots*), Diagrammatic Monte Carlo of the present work (*triangles*), the modified Feynman variational method (*solid curve*), the reduced Feynman variational method (*dotted curve*), the Momentum Average approximation  $MA^{(0)}$  (*dashed curve*) [12, 13], method of canonical transformations (*dot-dot-dashed curve*), and the RS perturbation theory [12, 13] (*short-dashed line*).

sufficiently small. Consequently, the polaron self-energy must be evaluated starting from a finite value of the coupling constant that ensures fulfillment of the variational inequality. In practice, this defines a practical lower bound on the coupling strength determined by the onset of numerical instability.

Increasing the number of lattice sites shifts this threshold to smaller values, ensuring convergence of the lattice polaron model toward the continuum limit. At the same time, the computational time scales as  $L^2$ . In the present calculations we use  $L = 40$ , for which the full-Feynman variational functional exhibits a stable minimum down to  $\lambda \approx 0.6$  for  $\omega_0 = 0.5$  and down to  $\lambda \approx 0.5$  for  $\omega_0 = 0.1$ . This practical lower bound on the coupling strength is not essential. As can be seen from Fig. 1 and, below, from Fig. 2, the full-Feynman ground-state energy at these coupling strengths is already extremely close to the weak-coupling

perturbation result. Moreover, the number of lattice sites can always be increased further, the only limitation being the computational cost.

As can be seen from Fig. 1, the full version of the modified Feynman variational method predicts the polaron ground-state energy very close to the Diagrammatic Monte Carlo results. In the strong-coupling regime, the variational ground-state energy obtained within the modified Feynman method is not asymptotically exact because of the parabolic form of the trial potential (as is also the case for the continuum polaron; see Refs. [35, 48]). Nevertheless, it yields ground-state energies extremely close to the exact numerical values obtained from Diagrammatic Monte Carlo calculations.

The reduced Feynman variational method, despite its simplicity, yields polaron ground-state energies that are only slightly higher than those obtained from the full formulation in the intermediate-coupling regime, spanning the crossover between the weak- and strong-coupling limits. The results of the reduced Feynman method are comparable to those of the full Feynman variational approach and diagrammatic Monte Carlo.

The momentum-average approximation [12, 13] performs reasonably well for the parameters chosen in Fig. 1. The variational results of the present work are of the same accuracy as the ground-state energy predicted by the momentum-average approximation. Moreover, in the intermediate and weak coupling range,  $\lambda \lesssim 1.5$ , the MA ground-state energy lies slightly above that predicted by perturbation theory, indicating a certain weakness of MA in this regime. In contrast, the modified Feynman method yields energies systematically lower than those obtained from perturbation theory and the method of canonical transformations.

Figure 2 shows the polaron ground-state energy for a lower phonon frequency,  $\omega_0 = 0.1t$ , for which Diagrammatic Monte Carlo data are also available [13, 14] for comparison, together with the results of different versions of the momentum-average approximation. In particular, the improved MA<sup>(2)</sup> scheme is included, which was designed to extend the applicability of MA to lower phonon frequencies.

As can be seen from Fig. 2, the modified Feynman variational method becomes more accurate than both MA<sup>(0)</sup> and MA<sup>(2)</sup> at lower phonon frequencies. MA was considered to be unsuitable at low phonon frequencies also for the double-well potential [51, 52]. The poor performance of MA in the intermediate and weak-coupling regime at  $\omega_0 = 0.1t$  is more pronounced than for  $\omega_0 = 0.5t$ , whereas the modified Feynman method remains in good agreement with Diagrammatic Monte Carlo results in both figures. This behavior can be

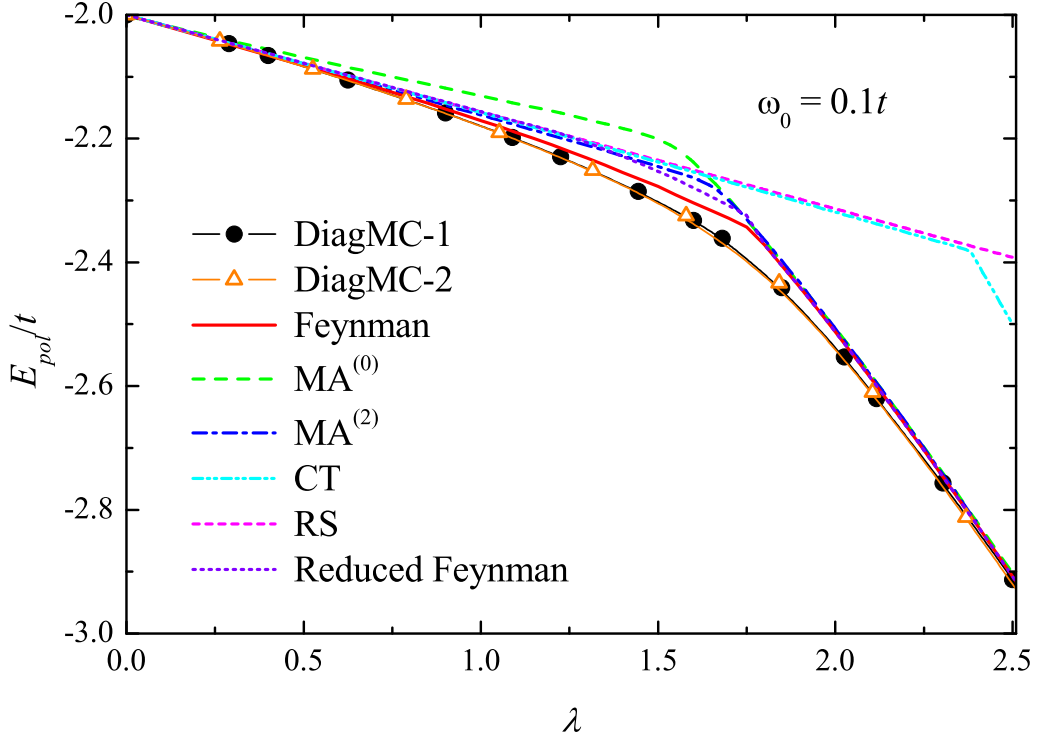


FIG. 2: Ground state energy of a Holstein polaron in 1D for  $\omega_0 = 0.1t$ , calculated by different methods: Diagrammatic Monte Carlo [12, 13] (*full dots*), Diagrammatic Monte Carlo of the present work (*triangles*), the modified Feynman variational method (*solid curve*), the reduced Feynman variational method (*dotted curve*), the momentum-average approximation  $MA^{(0)}$  and  $MA^{(2)}$  (*dashed and dot-dashed curves, respectively*) [12, 13], method of canonical transformations (*dot-dot-dashed curve*), and the RS perturbation theory [12, 13] (*short-dashed line*).

transparently understood from the fact that the modified Feynman variational method is not restricted to phonon frequencies that are not small compared to  $t$ , and explicitly reduces to the well-known Feynman approach for a continuum polaron in the adiabatic limit  $t \gg \omega_0$ . In addition, it is worth noting that both the full Feynman approximation and the reduced one provide lower polaron energies with respect to  $MA^{(0)}$  and  $MA^{(2)}$  for  $\omega_0 = 0.1t$ .

## 2. Polaron with spin-orbit coupling

For the ground-state energy of a single-band polaron, the full Feynman approximation exhibits numerically only a relatively small lowering of the polaron energy in the crossover region between the weak- and strong-coupling regimes compared to the reduced Feynman

approach. In this respect, the reduced Feynman approximation is particularly relevant for the polaron with spin–orbit coupling, because the validity of the full Feynman approach for a polaron described by a matrix Hamiltonian with complex matrix elements still requires careful examination.

Figure 3 shows the difference between the ground-state energy of a polaron with Rashba spin–orbit coupling and the free-electron ground-state energy  $E_0$  given by (14), using the parameters of Ref. [41]: phonon frequency  $\omega_0 = t$  and spin–orbit coupling potential  $V_s = 0$  (a) and  $V_s = t$  (b). The results are obtained using several approaches: the reduced Feynman variational method, the numerical calculation of Ref. [41] based on exact diagonalization (ED) of the electron–phonon Hamiltonian, the method of canonical transformations developed in the present work, Rayleigh–Schrödinger perturbation theory, and two variants of the Lang–Firsov approximation. The latter include the next-to-leading-order LF approximation described in Ref. [41],

$$E_{LF}^{(2)} - E_0 = -2t\lambda \left( 1 + 2 \frac{t^2 + V_s^2}{(2t\lambda)^2} \right), \quad (75)$$

and the leading-order term of the LF approximation,  $(-2t\lambda)$ . The coupling constant  $\lambda$  in the figure is rescaled by a factor  $1/\pi$  to allow a transparent comparison, so that  $\lambda$  is defined consistently in the present work and in Ref. [41].

As can be seen from Fig. 3, the validity of the variational inequality for the functional derived within the reduced Feynman approximation is numerically confirmed for the polaron with spin–orbit coupling. The variational polaron ground-state energy exhibits a continuous but non-smooth crossover between the weak- and strong-coupling regimes. In fact, the numerical calculation of Ref. [41] shows no polaron “phase transition” as the coupling constant is varied. Nevertheless, this artifact of the reduced Feynman variational method can be useful, as it clearly highlights the coupling strength range in which the polaron crosses over from the weak- to the strong-coupling regime.

The other analytic approximations shown in Fig. 3 yield results close to those obtained from the reduced Feynman approximation and from the numerical calculation in their respective regimes of validity. RS perturbation theory is applicable only in the weak-coupling regime. The Lang–Firsov approximation LF<sup>(2)</sup> performs well in the strong-coupling regime. The method of canonical transformations captures the entire range of coupling strengths, being asymptotically exact in the weak-coupling limit and equivalent to the leading-order

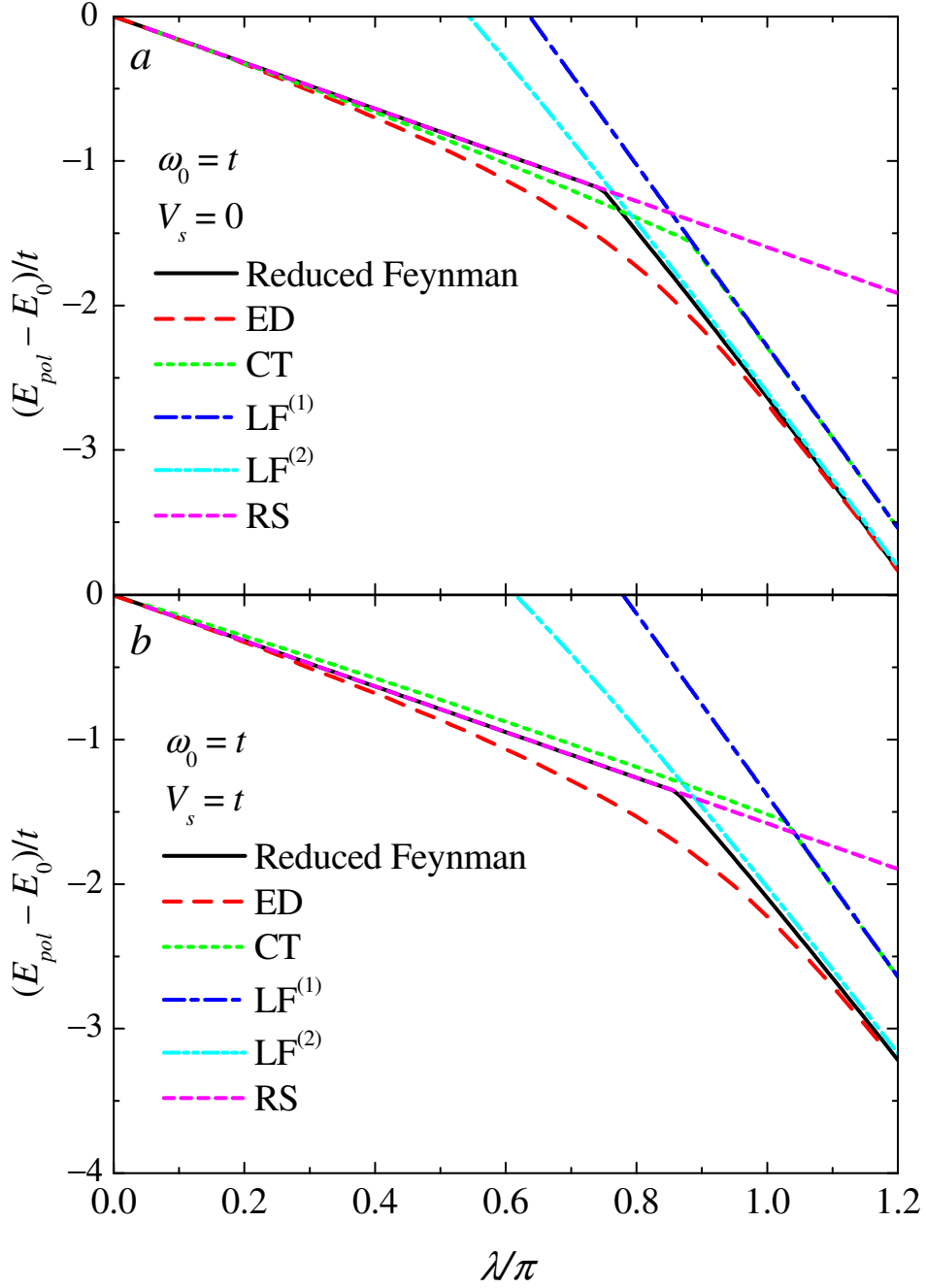


FIG. 3: Ground state energy of a polaron with the Rashba spin-orbit coupling with the phonon frequency  $\omega_0 = t$  and the SO potential  $V_s = 0$  (a) and  $V_s = t$  (b) calculated using different methods: the reduced Feynman approach (*solid curves*), the exact diagonalization method [41] (*dashed curves*), the method of canonical transformations (*dotted curves*), the RS perturbation theory (*dot-dashed curves*), the next-to-leading order (*dot-dot-dashed curves*) and leading-order (*short-dashed curves*) Lang-Firsov approximations.

Lang–Firsov approximation in the strong-coupling regime. For vanishing spin–orbit coupling, the method of canonical transformations yields a slightly lower ground-state energy than perturbation theory in the weak-coupling regime. For sufficiently strong spin–orbit coupling,  $V_s = t$ , the ground-state energy obtained from the method of canonical transformations lies slightly above the perturbative result.

Figure 4 displays the ground-state energy of a polaron with spin–orbit coupling in the adiabatic regime,  $\omega_0 = 0.1t$ , calculated within the reduced Feynman variational approach and compared with the numerical results of Ref. [41] and with the same analytic methods as in Fig. 3. As can be seen from the figure, in this regime the reduced Feynman approximation is highly accurate and exhibits good agreement with the numerical calculation over the entire range of coupling strengths. This behavior of the variational ground-state energy can be understood from the fact that the crossover region between the weak- and strong-coupling regimes narrows as the adiabatic ratio  $t/\omega_0$  increases.

Finally, we examine the dependence of the Rashba polaron ground-state energy on the spin–orbit coupling potential. In Fig. 5, the difference between the polaron ground-state energy obtained using the reduced Feynman method and the free-electron ground-state energy is compared with the momentum-average approximation MA<sup>(2)</sup> of Ref. [36] with  $\omega_0 = t$ . Overall, good agreement between the present variational results and the momentum average data is observed. The agreement is particularly good in the strong-coupling regime, which is reached in Fig. 5 for  $V_s \gtrsim 2t$ . In accordance with the observations of Ref. [36], we conclude that spin–orbit coupling effectively reduces the electron–phonon coupling strength, as evidenced by the crossover from the strong- to the weak-coupling regime upon increasing the spin–orbit coupling potential. The transition between the strong- and weak-coupling regimes occurs at  $V_s \approx 2.7$  for  $\lambda = 4$ , shifting to a lower value  $V_s \approx 0.6$  for  $\lambda = 2.5$ . For the smallest coupling constant  $\lambda = 1.5$ , the weak-coupling regime persists for all values of the SO potential.

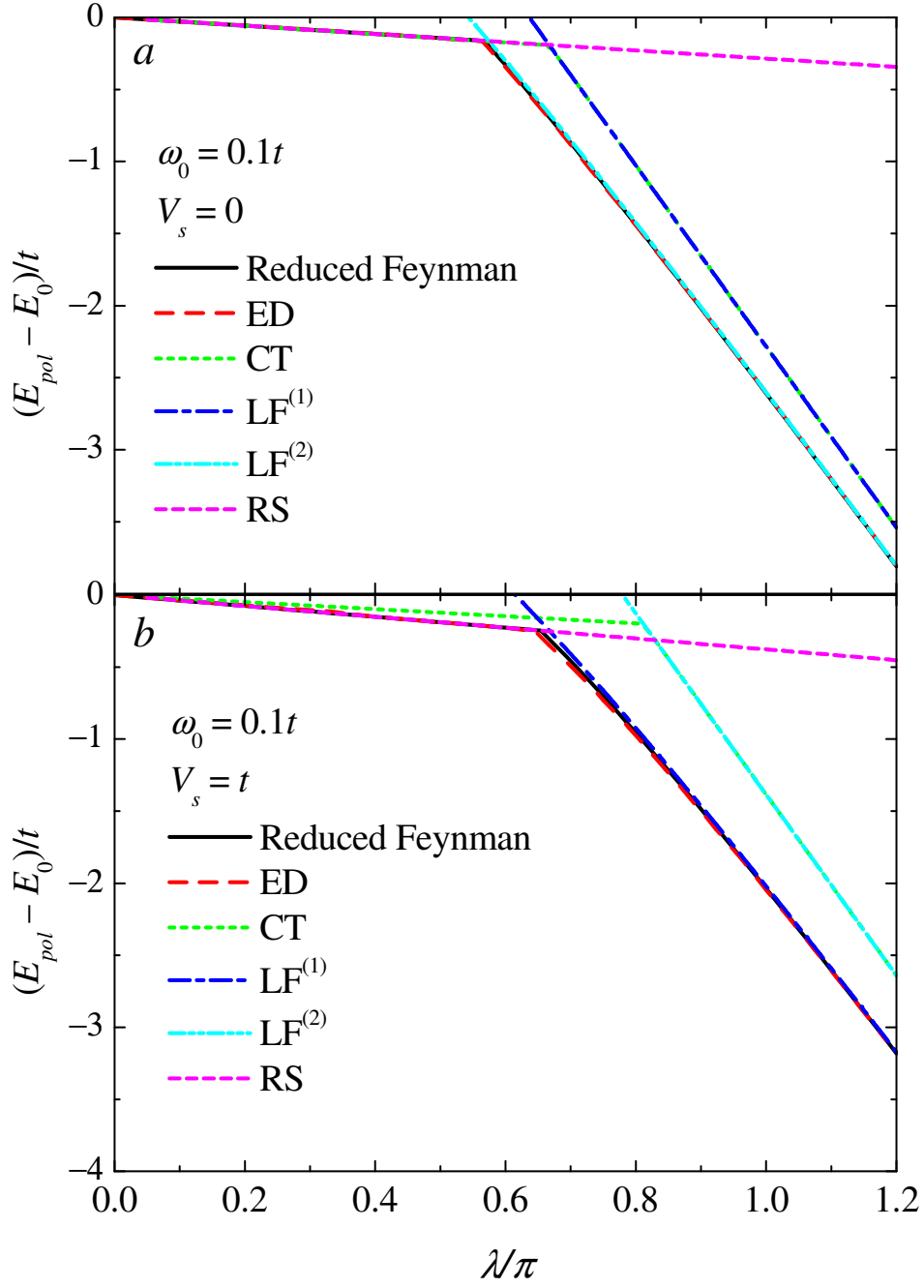


FIG. 4: Ground state energy of a polaron with the Rashba SO coupling with the phonon frequency  $\omega_0 = 0.1t$  and the SO potential  $V_s = 0$  (a) and  $V_s = t$  (b). The notations are the same as in Fig. 3.

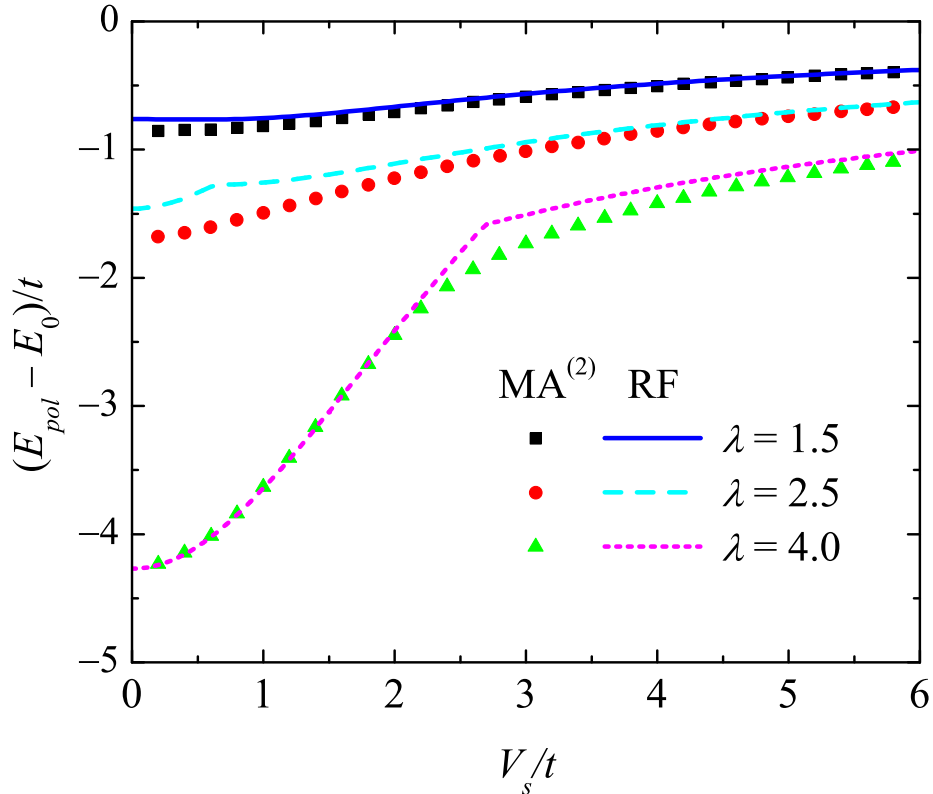


FIG. 5: Energy difference  $E_{pol} - E_0$  as a function of the SO coupling potential  $V_s$  for different values of the coupling strength  $\lambda$ . *Curves*: results of the calculation within the reduced Feynman approximation. *Symbols*: results of the momentum-average approximation  $MA^{(2)}$  [36].

## B. Polaron dispersion

### 1. Single band

Here, we analyze the polaron dispersion of a Holstein polaron in a single band, calculated using different analytic approximations.

Figure 6 shows the polaron dispersion throughout the Brillouin zone for the Holstein polaron in 1D with  $\omega_0 = t$ ,  $a_0 = 1$ , and  $\lambda = 1$ , obtained using different approximations: the Density Matrix Renormalization Group theory (DMRG) applied by Bonča *et al.* [40] (which appears to be numerically exact), the self-consistent Wigner-Brillouin approximation (WB) [12–15], the improved WB as described in the present work, the modified Feynman variational approach, the Rayleigh-Schrödinger perturbation theory, and the method of canonical transformations.

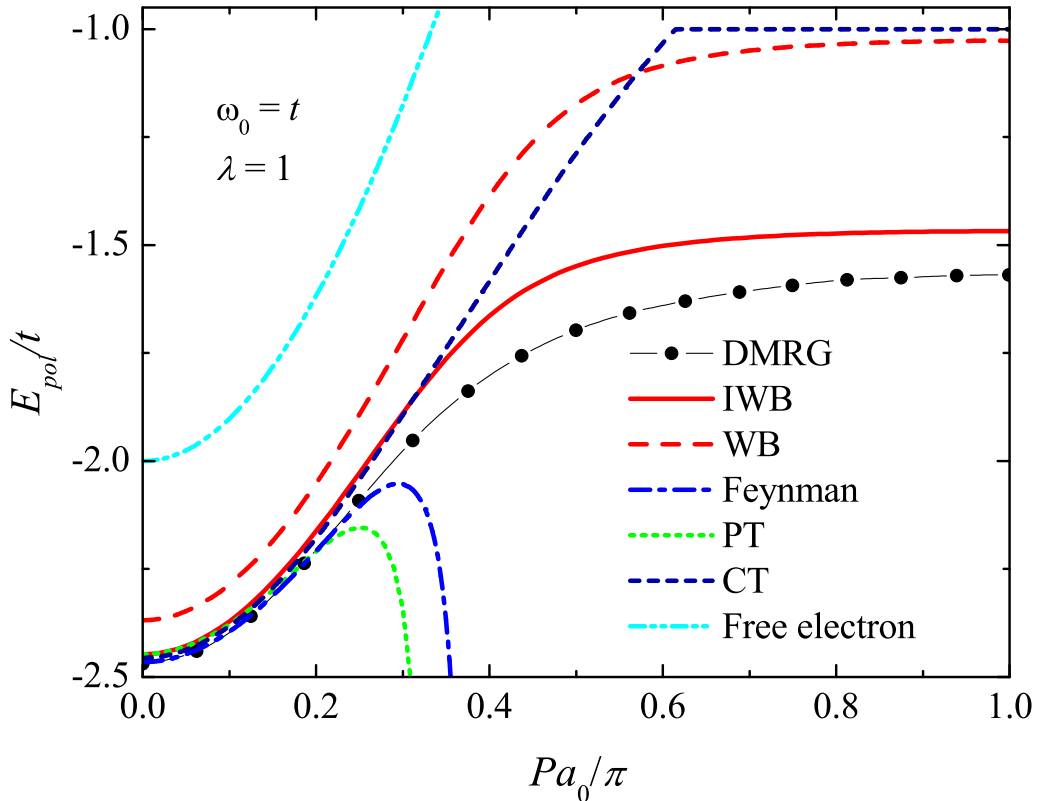


FIG. 6: Momentum-dependent polaron self-energy calculated for the Holstein polaron in 1D for  $\omega_0 = t$ ,  $a_0 = 1$  and  $\lambda = 1$  using different approximations. *Full dots*: Density Matrix Renormalization Group Theory. *Dashed red curve*: self-consistent Wigner-Brillouin approximation (WB). *Solid red curve*: improved WB. *Dot-dashed blue curve*: modified Feynman variational approach. *Dotted green curve*: Rayleigh-Schrödinger perturbation theory (RS). *Short-dashed blue curve*: method of canonical transformations (CT). *Dot-dot-dashed cyan curve*: the free-electron band energy.

First, it can be seen from Fig. 6 that the Rayleigh-Schrödinger perturbation theory fails to describe the polaron dispersion over the entire momentum range, being realistic only at small momenta. The reason is well known: the perturbative expression for the polaron self-energy at nonzero polaron momentum contains resonances when the momentum becomes sufficiently large.

A similar feature appears for the momentum-dependent polaron energy calculated within the modified Feynman variational approach, because the variational expression contains denominators analogous to those in RS, with the energies of the trial system replacing the free-electron band energies. Consequently, the momentum dependence of the polaron energy

within RS and within the modified Feynman variational approach is qualitatively similar, differing mainly quantitatively.

The self-consistent Wigner-Brillouin expression for the momentum-dependent polaron self-energy does not contain resonances, because the polaron energy appears both on the left-hand side and in the denominator on the right-hand side of the defining equation. The resulting polaron dispersion is therefore qualitatively realistic over the entire Brillouin zone. However, the polaron energy within WB is everywhere higher than that obtained within RS, as noted in many works, in particular in Ref. [28].

In order to improve WB while retaining its ability to describe the polaron dispersion over the full momentum range, Lindemann [31] and Gerlach and Smondyrev [32] proposed a modified WB-like approach that is variationally correct and reproduces a Tamm-Dankoff-type procedure by regrouping the unperturbed and interaction Hamiltonians, as described in Subsec. II B 2. This improved WB matches RS at zero momentum and yields a polaron dispersion over the entire Brillouin zone. As can be seen from Fig. 6, the improved WB method gives the polaron self-energy much closer to the DMRG results than all other approximations considered in the present work.

Finally, we also plot in the same figure the polaron self-energy obtained within the CT approach. While it is rather close to the DMRG results at small momentum (performing better than RS and the modified WB), it shows relatively poor agreement at large momentum. In particular, it exhibits a non-smooth behavior corresponding to the transition between weak-coupling and strong-coupling regimes, already indicated above.

It is also instructive to examine the polaron self-energy in the small-momentum range, as shown in Fig. 7. As can be seen from the figure, the non-improved WB polaron energy at small momentum is higher than that provided by the other approximations. The perturbation theory and the improved Wigner-Brillouin approximation yield self-energies that tend to the same limit as  $P \rightarrow 0$ . The polaron self-energy obtained within the method of canonical transformations at small  $P$  is slightly lower than the perturbative result.

Remarkably, the Feynman variational approach at small momentum is in good agreement with the Density Matrix Renormalization Group theory. This is consistent with the agreement between the Feynman approach and the Diagrammatic Monte Carlo calculations for the ground-state energy presented in Subsec. III A.

We also refer to the numerically exact calculations of the momentum-dependent polaron

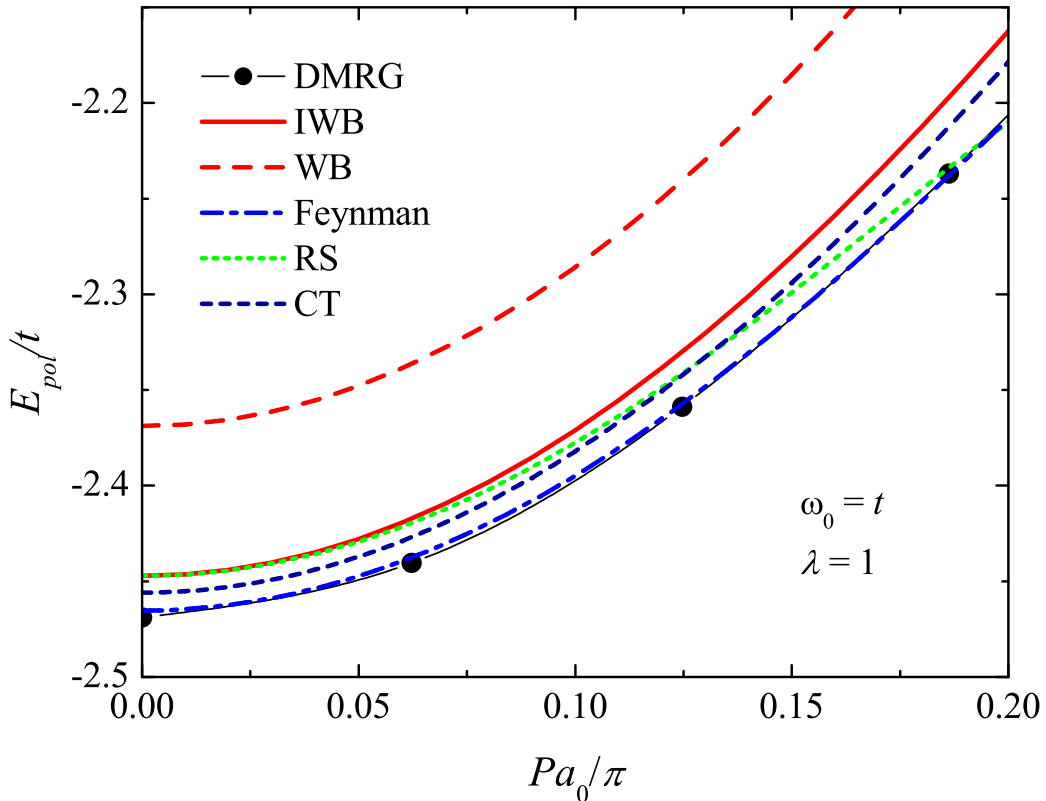


FIG. 7: Momentum-dependent polaron self-energy from Fig. 6 in the small momentum range. The notations are the same as in Fig. 6.

self-energy by Wellein and Fehske [39] for comparison with our results. Figure 8 shows the polaron dispersion for the one-dimensional Holstein model with different phonon frequencies at the coupling strength  $\lambda = 0.1$ , calculated within the improved (solid curves) and standard Wigner-Brillouin approximations. The symbols represent data points from the numerically exact calculations [39].

As can be seen from Fig. 8, the improved Wigner-Brillouin approximation is in good agreement with the numerically exact results, and performs systematically better than the standard WB. In addition, a subtle feature of the dispersion is correctly reproduced: at  $P = 0$  the polaron self-energy decreases with increasing  $\omega_0$ , whereas at sufficiently large momentum the self-energy increases as  $\omega_0$  increases. This agreement between analytic and numerical results demonstrates that the WB procedure removes resonances in a physically correct manner.

In Fig. 9, a comparison between analytic and numerical simulations of the momentum-

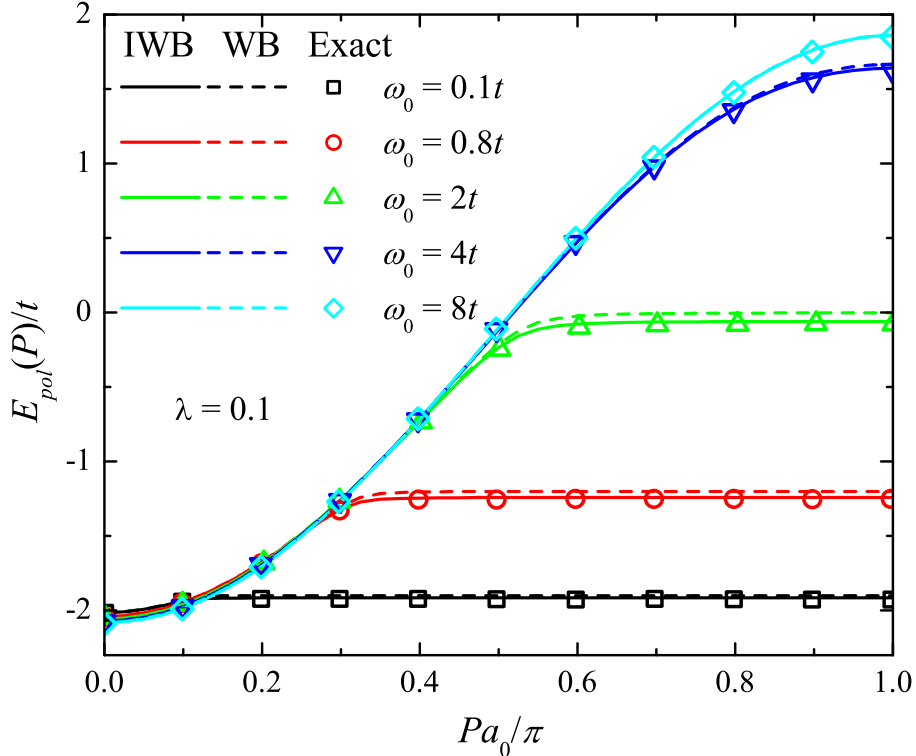


FIG. 8: *Symbols*: exact results for the polaron band dispersion of the 1D Holstein model with  $\lambda = 0.1$  and several phonon frequencies calculated in Ref. [39] for a finite lattice with 20 sites. *Solid and dashed curves*: results obtained within, respectively, the improved and standard Wigner-Brillouin approximation.

dependent polaron energy is shown for the same model as in the previous figure, at a stronger coupling  $\lambda = 0.5$  and  $\omega_0 = 0.8t$ . For this coupling strength, a small discrepancy appears between the exact numerical results and those provided by the improved Wigner-Brillouin method. The standard WB approximation (dashed curve) performs poorly at this coupling strength. In summary, the improved WB approximation appears promising for the description of the polaron dispersion, at least in the range of weak and intermediate coupling strength.

#### IV. CONCLUSIONS

In this work, we have developed, extended, and systematically benchmarked a set of analytic approaches for the polaron problem in a finite-width, nonparabolic conduction band,

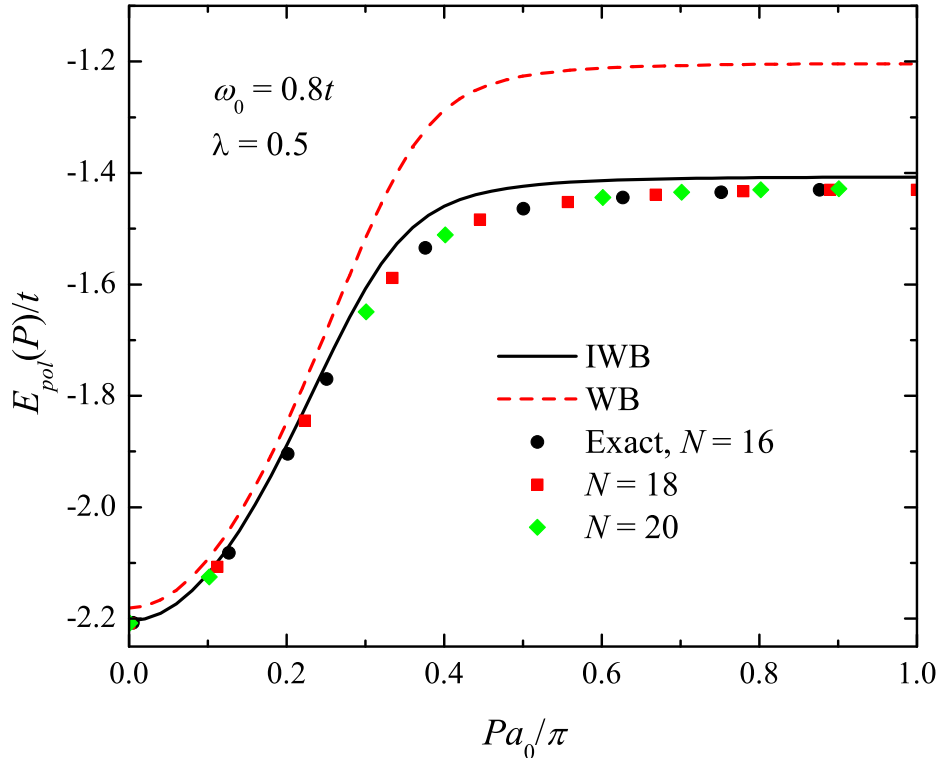


FIG. 9: *Symbols*: exact results for the polaron band dispersion of the 1D Holstein model with  $\lambda = 0.4$  and  $\omega_0 = 0.8t$  [39] for a finite lattice with 16, 18 and 20 sites. *Solid and dashed curves* show results of the present calculation within, respectively, the improved and standard Wigner-Brillouin approximation.

with particular emphasis on tight-binding dispersions and on the interplay between electron-phonon coupling and spin-orbit interaction. The central motivation of this study was to reassess the status of well-established continuum polaron methods when the effective-mass approximation breaks down, and to construct an analytic framework that remains reliable across weak, intermediate, and strong coupling regimes without relying on uncontrolled assumptions.

A first important outcome of our analysis is that several approaches traditionally regarded as “weak-coupling” methods exhibit a substantially broader range of validity when reformulated for a finite-bandwidth lattice polaron. In particular, the self-consistent Wigner-Brillouin approximation and its improved, variationally consistent variant provide a momentum-dependent polaron self-energy that is free of resonance divergences throughout the entire Brillouin zone. The improved Wigner-Brillouin scheme exactly reproduces

Rayleigh–Schrödinger perturbation theory at zero momentum and yields a polaron dispersion in good agreement with numerically exact results at weak coupling, while remaining qualitatively reliable up to intermediate coupling strengths. This makes it a powerful analytic tool for addressing polaron band renormalization, a regime where bare perturbation theory inevitably fails.

The method of canonical transformations turns out to be particularly revealing in the lattice context. While its continuum counterpart, the Lee–Low–Pines approach, is strictly limited to weak coupling, its extension to a tight-binding band unexpectedly captures both weak- and strong-coupling limits. In the strong-coupling regime, the method becomes exactly equivalent to the leading-order Lang–Firsov approximation, thereby providing a single analytic construction that interpolates between qualitatively distinct physical regimes. The appearance of a non-smooth crossover associated with competing variational minima reflects an intrinsic limitation of the method, but at the same time offers a clear physical interpretation of self-trapping phenomena on a lattice and clarifies why such behavior is absent in the continuum limit.

The central result of the present work is the extension of the Feynman variational principle to polarons in nonparabolic, finite-width conduction bands. We have shown that the Feynman approach can be reformulated without requiring explicit knowledge of the kinetic-energy functional, by working entirely in momentum space and by treating the trial system exactly. This resolves a long-standing conceptual obstacle that had previously restricted the applicability of the Feynman variational method to parabolic dispersions. The resulting variational functional yields a rigorous upper bound for the polaron ground-state energy and, at the same time, provides access to the full momentum dependence of the polaron dispersion.

A detailed comparison with numerically exact methods demonstrates that the modified Feynman variational approach reproduces Diagrammatic Monte Carlo results for the ground state energy with high accuracy over the entire range of coupling strengths. Its advantage over the Momentum Average approximation becomes particularly pronounced at low phonon frequencies, where MA requires increasingly elaborate refinements to maintain quantitative accuracy. In contrast, the present approach remains uniformly reliable and smoothly approaches the adiabatic limit, analytically reducing to the exact Feynman solution for a continuum polaron as the bandwidth increases. This uniform performance

across weak, intermediate, and strong coupling, as well as across adiabatic and nonadiabatic regimes, constitutes one of the main strengths of the method.

For polarons with Rashba spin–orbit coupling, we have shown that the reduced Feynman variational approach remains rigorously justified and yields ground-state energies in good agreement with numerically exact calculations. The method correctly captures the effective reduction of the electron–phonon coupling induced by spin–orbit interaction and reproduces the continuous crossover between weak and strong coupling as functions of both the electron–phonon and spin–orbit coupling strengths. Comparison with Diagrammatic Monte Carlo data confirms the quantitative reliability of the approach, particularly in the adiabatic and strong-coupling regimes, where competing analytic methods become less controlled. The extension of the analytical framework to polarons with Rashba-type spin-orbit coupling provides a stringent test of the methods in the presence of nontrivial band topology and complex matrix Hamiltonians, confirming their robustness beyond single-band models.

Beyond its quantitative success, the present formulation of the Feynman variational method has a broader methodological significance. It provides a consistent and flexible framework for treating polarons in arbitrary lattice bands, independent of the specific form of the electron–phonon interaction or phonon dispersion. The approach can be straightforwardly extended to finite temperatures, to multiband systems, and to more general forms of spin–orbit coupling. It also opens the way to controlled treatments of nonlinear electron–phonon interactions and to calculations of dynamical response functions, such as the polaron optical conductivity, in direct analogy with earlier continuum studies.

In summary, the results presented here demonstrate that the Feynman variational principle, when properly reformulated, remains one of the most powerful and versatile analytic tools for the polaron problem. Its extension to nonparabolic, finite-width conduction bands closes an important conceptual gap between continuum and lattice polaron theories and provides a unified analytic description that is competitive with state-of-the-art numerical methods across a wide range of physically relevant regimes.

### **Acknowledgments**

We are grateful to Mona Berciu for Diagrammatic Monte Carlo and momentum-average data used for the comparison with the analytic predictions of the present work. S.K., M.H.

and J.T. acknowledge the Research Foundation Flanders (FWO), file numbers 1224724N and V472923N, for their funding of this research. C.F., J.T., S.R. and T.H. acknowledge support from the joint Austrian Science Fund (FWF) - FWO project 10.55776/PIN5456724. A.S.M. and S.R. acknowledge support from the Croatian Science Foundation (HRZZ) under the project No. IP-2024-05-2406. L.C. acknowledges the Vienna Doctoral School of Physics. Our Diagrammatic Monte Carlo computational results presented in this article were obtained using the Austria Scientific Cluster (ASC).

### Data availability statement

The numerical data supporting the findings of this work are publicly available in [53].

- 
- [1] L.D. Landau, “*Electron motion in crystal lattices*”, Phys. Z. Sowjetunion **3**, 664 (1933).
  - [2] H. Fröhlich, “*Electrons in lattice fields*”, Adv. Phys. **3**, 325 (1954).
  - [3] T. Holstein, “*Studies of polaron motion: Part I. The molecular-crystal model*”, Ann. Phys. **8**, 325 (1959).
  - [4] T. Holstein, “*Studies of polaron motion: Part II. The “small” polaron*”, Ann. Phys. **8**, 343 (1959).
  - [5] R. P. Feynman, “*Slow Electrons in a Polar Crystal*”, Phys. Rev. **97**, 660 (1955).
  - [6] R. P. Feynman, *Statistical Mechanics* (New York: Benjamin, 1972).
  - [7] C. Franchini, M. Reticcioli, M. Setvin, and U. Diebold, “*Polarons in Materials*”, Nat. Rev. Mater. **6**, 560 (2021).
  - [8] Y. E. Shchadilova, F. Grusdt, A. N. Rubtsov, and E. Demler, “*Polaronic mass renormalization of impurities in Bose-Einstein condensates: Correlated Gaussian-wave-function approach*”, Phys. Rev. A **93**, 043606 (2016).
  - [9] A. Ahsin, I. Ejaz, S. Sarfaraz, K. Ayub, and H. Ma, “*Polaron Formation in Conducting Polymers: A Novel Approach to Designing Materials with a Larger NLO Response*”, ACS Omega **9**, 14043 (2024).
  - [10] H. Tajima, H. Moriya, W. Horiuchi, E. Nakano, and K. Iida, “*Polaronic proton and diproton clustering in neutron-rich matter*”, Phys. Lett. B **851**, 138567 (2024). DOI:

<https://doi.org/10.1016/j.physletb.2024.138567>

- [11] L. Celiberti *et al.*, “*Spin-orbital Jahn-Teller bipolarons*”, Nat. Commun. **15**, 2429 (2024).
- [12] M. Berciu, “*Green’s Function of a Dressed Particle*”, Phys. Rev. Lett. **97**, 036402 (2006).
- [13] G. L. Goodvin, M. Berciu, and G. A. Sawatzky, “*Green’s Function of the Holstein Polaron*”, Phys. Rev. B **74**, 245104 (2006).
- [14] M. Berciu and G. L. Goodvin, “*Systematic improvement of the momentum average approximation for the Green’s function of a Holstein polaron*”, Phys. Rev. B **76**, 165109 (2007).
- [15] M. Bhattacharya, A. Chatterjee, and T. K. Mitra, Phys. Letters A **134**, 391 (1989).
- [16] I. G. Lang and Yu. A. Firsov, Zh. Eksp. Teor. Fiz. **43**, 1843 (1962) [Sov. Phys. JETP **16**, 1301 (1963)].
- [17] S. I. Pekar, *Untersuchungen über die Elektronentheorie der Kristalle* (Akademie-Verlag, Berlin, 1954).
- [18] V. Cataudella, G. De Filippis, and G. Iadonisi, “*Variational approach for the Holstein molecular-crystal model*”, Phys. Rev. B **60**, 15163 (1999).
- [19] V. Cataudella, G. De Filippis, and G. Iadonisi, “*Polaron features of the one-dimensional Holstein molecular crystal model*”, Phys. Rev. B **62**, 1496 (2000).
- [20] D. Jansen, J. Bonča, and F. Heidrich-Meisner, “*Finite-temperature density-matrix renormalization group method for electron-phonon systems: Thermodynamics and Holstein-polaron spectral functions*”, Phys. Rev. B **102**, 165155 (2020).
- [21] Paul J. Robinson, Ian S. Dunn, David R. Reichman, “*Cumulant methods for electron-phonon problems. I. Perturbative expansions*”, Phys. Rev. B **105**, 224304 (2022).
- [22] Paul J. Robinson, Ian S. Dunn, David R. Reichman, “*Cumulant methods for electron-phonon problems. II. The self-consistent cumulant expansion*”, Phys. Rev. B **105**, 224305 (2022).
- [23] T. D. Lee, F. E. Low, and D. Pines, “*The Motion of Slow Electrons in a Polar Crystal*”, Phys. Rev. **90**, 297 (1953).
- [24] S. Barišić, J. Labbé, and J. Friedel, “*Tight binding and transitionmetal superconductivity*”, Phys. Rev. Lett. **25**, 919 (1970).
- [25] S. Barišić, “*Rigid-atom electron-phonon coupling in the tight-binding approximation. I*”, Phys. Rev. B **5**, 932 (1972).
- [26] S. Barišić, “*Self-consistent electron-phonon coupling in the tight-binding approximation. II*”, Phys. Rev. B **5**, 941 (1972).

- [27] W. P. Su, J. R. Schrieffer, and A. J. Heeger, “Solitons in polyacetylene”, Phys. Rev. Lett. **42**, 1698 (1979).
- [28] D. J. J. Marchand, G. De Filippis, V. Cataudella, M. Berciu, N. Nagaosa, N. V. Prokof’ev, A. S. Mishchenko and P. C. E. Stamp, “*Sharp transition for single polarons in the one-dimensional Su-Schrieffer-Heger Model*”, Phys. Rev. Lett. **105**, 266605 (2010).
- [29] B. Lau, M. Berciu, and G. A. Sawatzky, “*Single-polaron properties of the one-dimensional breathing-mode Hamiltonian*”, Phys. Rev. B **76**, 174305 (2007).
- [30] G. L. Goodvin and M. Berciu, “*Momentum average approximation for models with electron-phonon coupling dependent on the phonon momentum*”, Phys. Rev. B **78**, 235120 (2008).
- [31] G. Lindemann, R. Lassnig, W. Seidenbusch, and E. Gornik, “*Cyclotron resonance study of polarons in GaAs*”, Phys. Rev. B **28**, 4693 (1983).
- [32] B. Gerlach and M. A. Smondyrev, “*Upper and lower bounds for the large polaron dispersion in 1, 2, or 3 dimensions*”, Phys. Rev. B **77**, 174303 (2008).
- [33] A. S. Alexandrov and P. E. Kornilovitch, “*Mobile Small Polaron*”, Phys. Rev. Lett. **82**, 807 (1999).
- [34] E. I. Rashba, “*Properties of semiconductors with an extremum loop .1. Cyclotron and combi-national resonance in a magnetic field perpendicular to the plane of the loop*”, Fizika Tverd. Tela, **2**, 1224 (1960) [English translation: Sov. Phys. Solid State **2**, 1109 (1960)].
- [35] A. S. Mishchenko, N. V. Prokof’ev, A. Sakamoto, and B. V. Svistunov, “*Diagrammatic quantum Monte Carlo study of the Fröhlich polaron*”, Phys. Rev. B **62**, 6317 (2000).
- [36] L. Covaci and M. Berciu, “*Polaron Formation in the Presence of Rashba Spin-Orbit Coupling: Implications for Spintronics*”, Phys. Rev. Lett. **102**, 186403 (2009).
- [37] S. Ragni, T. Hahn, Z. Zhang, N. Prokof’ev, A. Kuklov, S. Klimin, M. Houtput, B. Svistunov, J. Tempere, N. Nagaosa, C. Franchini, and A. S. Mishchenko, “*Polaron with Quadratic Electron-phonon Interaction*”, Phys. Rev. B **107**, L121109 (2023).
- [38] S. N. Klimin, J. Tempere, M. Houtput, S. Ragni, T. Hahn, C. Franchini, and A. S. Mishchenko, “*Analytic method for quadratic polarons in nonparabolic bands*”, Phys. Rev. B **110**, 075107 (2024).
- [39] G. Wellein and H. Fehske, “*Polaron band formation in the Holstein model*”, Phys. Rev. B **56**, 4513 (1997).
- [40] J. Bonča, S. A. Trugman, and I. Batistić, “*Holstein polaron*”, Phys. Rev. B **60**, 1633 (1999).

- [41] Z. Li, L. Covaci, M. Berciu, D. Baillie, and F. Marsiglio, “*Impact of spin-orbit coupling on the Holstein polaron*”, Phys. Rev. B **83**, 195104 (2011).
- [42] A. L. Fetter and J. D. Walecka, *Quantum Theory of Many-Particle Systems*, (McGraw-Hill, New York, 1971; Dover, Mineola, NY, 2003).
- [43] K. E. Cahill and R. J. Glauber, Phys. Rev. **177**, 1857 (1969).
- [44] J. T. Devreese and A. S. Alexandrov, “*Fröhlich polaron and bipolaron: recent developments*”, Rep. Prog. Phys. **72**, 066501 (2009).
- [45] S. T. Epstein, in *Perturbation Theory and its Applications in Quantum Mechanics*, edited by C. H. Wilcox (Wiley, New York, 1966), p. 49.
- [46] N. N. Bogolubov and N. N. Bogolubov, Jr., *Some Aspects of Polaron Theory* (World Scientific, Singapore, 1988).
- [47] J. T. Devreese and F. Brosens, “*Extension to the case of a magnetic field of Feynman’s path-integral upper bound on the ground-state energy: Application to the Fröhlich polaron*”, Phys. Rev. B **45**, 6459 (1992).
- [48] S. J. Miyake, “*The Ground State of the Optical Polaron in the Strong-Coupling Case*”, J. Phys. Soc. Jpn. **41**, 747 (1976).
- [49] J. Devreese, J. De Sitter, and M. Goovaerts, “*Optical Absorption of Polarons in the Feynman-Hellwarth-Iddings-Platzman Approximation*”, Phys. Rev. B **5**, 2367 (1972).
- [50] S. N. Klimin, J. Tempere, and J. T. Devreese, “*All-coupling polaron optical response: Analytic approaches beyond the adiabatic approximation*”, Phys. Rev. B **94**, 125206 (2016).
- [51] C. P. J. Adolphs and M. Berciu, “*Single-polaron properties for double-well electron-phonon coupling*”, Phys. Rev. B **89**, 035122 (2014)
- [52] S. Ragni, T. Miškić, T. Hahn, N. Prokof’ev, O. S. Barišić, N. Nagaosa, C. Franchini, and A. S. Mishchenko, “*Polarons with arbitrary nonlinear electron-phonon interaction*”, Phys. Rev. Research **7**, 043304 (2025).
- [53] S. N. Klimin, *Analytic treatment of a polaron in a nonparabolic conduction band* [Dataset], Zenodo (2026), doi:[10.5281/zenodo.18816304](https://doi.org/10.5281/zenodo.18816304)